A THESIS
FOR THE DEGREE OF DOCTOR OF PHILOSOPHY

A Study of high-T_c Superconductor Submicron Josephson Junction Devices

Shrikant Saini

Department of Mechanical System Engineering

GRADUATE SCHOOL

JEJU NATIONAL UNIVERSITY

2011. 08

博士學位論文

A Study of high-T_c Superconductor Submicron Josephson Junction Devices

濟州大學校 大學院

機械工學科

사이니 스리칸트

2011 年 8 月

A Study of High-T_c Superconductor Submicron Josephson Junction Devices

Shrikant Saini

(Supervised by Professor Sang-Jae Kim & Professor Gui Shik Kim)

A thesis submitted in partial fulfillment of the requirement for the degree of

Doctor of Philosophy

2011. 08

The thesis has been examined and approved.

Thesis Director, Prof. Soon-Gul Lee,	Department of Display and Semiconductor Physics, Korea University
Thesis Committee Member, Prof. Heon-Ju Lee,	Department of Nuclear Energy Engineering, Jeju National University
Thesis Committee Member, Prof. Young-Sun Mok,	Department of Chemical Engineering, Jeju National University
Thesis Committee Member, Prof. Gui Shik Kim,	Department of Mechanical Engineering, Jeju National University
Thesis Committee Member, Prof. Sang-Jae Kim,	Department of Mechatronics Engineering, Jeju National University

August, 2011.
Date

Department of Mechanical System Engineering
GRADUATE SCHOOL
JEJU NATIONAL UNIVERSITY
REPUBLIC OF KOREA

dedicated to

my lab

&

100^{th} anniversary of superconductivity

ACKNOWLEDGEMENTS

This thesis is a result of four year experimental research on submicron Josephson junctions devices on high T_c superconductors. The content of the thesis are always censored in a sense that only the success stories are told. The preliminary work, such as the numerous discussions concerning the ultra-small devices, the wiring of a cryostat, the days of lab shifting, the FIB breakdown, and installation of CCR is carefully filtered out during the writing of the thesis. Unfortunately these are the aspects that made my PhD period as it was: instructive, intensive, exciting, exhaustive, frustrating, fascinating, but most of the time I simply enjoyed it.

I would like to thank to my Prof. Sang-Jae Kim for supervising and introducing me about the field of quantum application of Josephson junctions. His enthusiasm concerning quantum physics application inspired me enormously. I appreciate the freedom you gave me to explore myself. Your truly scientific intuition has made you as a constant oasis of ideas and passions in science, which exceptionally inspire and enrich my growth as a student, a researcher and a scientist want to be. I am indebted to you more than you know.

I would also like to thank my research co-supervisor Prof. Gui Shik Kim for his continuous support during my Ph.D. work. I appreciate the collaboration work with Prof. Mukaida and Dr. Takamura for providing us the thin films which were used in a part of this study. Thanks to Prof. Yu. I. Latyshev and Prof. Hu-Jong Lee for the fruitful discussion of physics. I also want to thank to department Professors for their support.

I am of course also indebted to the members of the group, past and present for their combined help and support throughout the past few years, especially my batch mate, lab mate and roommate Guna, I thankful to you for your scientific & moral guidance during this Ph.D. time period. I would like to take the name of Mr Sang-Yul Oh who

taught me about the measurements and FIB operation in starting of PhD days. Thanks to Dr Rajneesh for scientific discussion during the lab stay. Karthi, I will never forget the humours and your PUNCHs! Further I want to mention my lab mates who provide me a good working environment to precede the different projects; thanks Dae Yong Kim, So Yoon Shin, Seong Jin Hong, Eui-Yong Hong, Tae Hyeon Kim, Seo Hyeon Park, Myeon Yeon Cho, Kwang Yool Ko, Jaeeon Seo, Sena Ko, Jong Up Yoon, Seong Tae Song. My lab is the most pleasant place with friendly lab mates I have ever worked.

Tea break is one of the good platforms for the research and physics. I thank to my tea break friends Dr. Anil, Dr. Saha, Dr. Ahsan, Khalid, Nauman, Murtuza, Naeem. Jeju might be lonely if you all were not here to make a perfect time; thanks to Dr. Hari, Dr. Ganesh, Dr. Navamathavan, Shanu, Purushi, Saranya, Anji, Sueng Hyun, Dr. Mahanama, Dr. Mahinda, Nandeesh, Uma, Ganesh Thanga, Sridharan, Dr. Gandhi, Dr. Neelesh, Chandran, Naveneethan, Ahmer bhai, Arshad, Rahul, Jack and many more.

I am also grateful for the Research Instruments Center (RIC) at Jeju National University for providing me opportunities to handle many instrument facilities during my study and I thank Mr. Jeong Eun Koh, Mr. Sang Hyeong Lee and Mrs. In Sil Yang at RIC for their cheerful assistance in the work. Many thanks to Graduate school which has been grateful to waive off the tuition fee for my doctoral studies. I also thank Brain Korea 21 (BK-21) project research grant which provided the funds for my entire Ph.D. work.

Sincere thanks to Prof. R. C. Budhani, Prof. S. Patnaik, and Dr. Shripal for their moral and academic support. Distance do not matter for the support is proven by Dr. S. D. Kaushik, Dr. Shekhar, Dr. Shalendra, Dr. Kartik Senapati, Dr. Navneet, Dr. Rajeeb Rakhit, Dr. Saumyadeep, Dr. Saumen Mandel, Dr. P. K. Muduli, Dr. Saurab, Rajeev Sharma, Ashok, Gyanu, Akhilesh and many more.

Nyamaa, a special thanks to you for being with me in the all ups and downs during the PhD.

This acknowledgement cannot be complete without mentioning the gratitude to my honorable parents for their belief in me and I'm unable to find proper words to express my feelings. I would like to take the name of my grandfather Dr. V. Prasad, Mr. Sovaranlal Saini and my father Mr. Aditya Kumar Saini for their unconditional support, understanding, and dedication throughout these years.

ABSTRACT

The non-linear current-voltage characteristics of Josephson effect phenomenon is always being focused by scientists and engineers. Using Josephson junction phenomenon with high-T_c superconductors gives a wide scope of applications. Depending on in-plane size, the application of Josephson junctions varied from the terahertz (THz) oscillator to the single electron transistors. This thesis is focused on the study of submicron Josephson junctions. The unit cell of layered high-T_c superconductors show intrinsic Josephson junctions (IJJs) phenomenon. The Cooper pair tunneling in the IJJs can be affected by quantum phase fluctuations when the resistance of a submicron stack is in the range of quantum resistance. To observe this quantum effect, we have fabricated stacks of IJJs of various in-plane area from 4 μm^2 down to 0.16 μm^2 in $Bi_2Sr_2CaCu_2O_{8+\delta}$ single crystal whiskers using three-dimensional focused ion beam (3-D FIB) etching technique. For stacks of in-plane area less than 1 μm^2 a strong suppression in critical current density (J_c) was noticed in current-voltage characteristics at 30 K. The possible mechanisms for this suppression of J_c are discussed and the data analysis points to the quantum phase fluctuations as the most likely mechanism of this effect. We have achieved quantum fluctuations at 30 K first time ever reported for $Bi_2Sr_2CaCu_2O_{8+\delta}$ (Bi-2212) single crystal whisker.

A-axis oriented thin films of $YBa_2Cu_3O_7$ are potentially superior to *c*-axis films for sandwich-type junction applications because of the larger coherence length in *a*-axis direction. Thus growth of thin epitaxial insulators or normal barriers on *a*-axis films, followed by another *a*-axis superconductor, is an important goal. Considering this phenomenon, we have studied a submicron stack of $YBa_2Cu_3O_7$ and $PrBa_2Cu_3O_7$ (Y123/Pr123) multi layered thin film Josephson junction. The dimensions of submicron stack is about 300 nm $\times$ 200 nm with the height of about 200 nm. The submicron stack shows the transi-

tion temperature about 84 K and critical current of about 0.12 mA at 30 K. We noticed the suppression in critical current as the effect of external microwave at different power. As we increase the power, the superconducting state was suppressed and resulted in the suppression of the critical current. However, we have not observed any voltage steps in current-voltage characteristics with external microwave irradiation.

Further we have fabricated a superconducting quantum interface device SQUID using focused ion beam etching technique. The microwave induced voltage steps are observed in I-V characteristics. The super current branch become resistive above a certain microwave power and the value of J_c was suppressed as we increased the microwave power. The power dependence of voltage steps shows the number of Josephson junctions contributing to the vortices-flow varies with the power of microwave. The formation of superconducting-semiconducting-superconducting -like Josephson junction is confirmed by Ambegaokar-Baratoff theory.

초록

조셉슨 효과의 비선형 전류-전압 특성은 지금까지 많은 과학자와 엔지니어들에게 연구 및 실험의 대상이 되어오고 있다. 고온 초전도체를 이용하여 제작한 조셉슨접합에 의한 양자현상을 이용하는 것은 매우 다양하고 폭 넓은 응용분야를 가지고 있다. 면내 (*in-plane*)크기에 따른 특성에 의존하는 조셉슨 접합은 THz 발진기에서부터 단전자트랜지스터에 이르기까지 응용분야가 매우 다양하다.

본 연구에서는 서브마이크론크기의 자연적으로 형성된 고온초전도체의 적층구조를 가공한 고유조셉슨접합(intrinsic Josephson junction)을 제작하고 그 기초물성 및 응용에 관한 연구를 수행하였다. 적층구조 고온초전도체의 단위층간에 수직방향으로 전류가 인가되면, 직렬로 연결된 층의 수에 비례한 전류-전압특성을 나타내는데, 이러한 접합을 고유조셉슨접합 혹은 고유조셉슨현상이라고 부른다.

고유조셉슨접합내의 쿠퍼쌍 턴넬은 적층구조접합의 저항이 양자저항보다도 크게 되면 양자페이즈(quantum phase)의 요동에 의한 영향을 받게 된다. 양자현상의 영향을 관찰하기 위하여 $Bi_2Sr_2CaCu_2O_{8+\delta}$ (Bi-2212) 수염상단결정에 입체적인(3-D) 집속이온빔가공을 이용하여 4 μm^2 에서 0.16 μm^2 에 이르는 다양한 면내크기의 고유조셉슨접합을 제작하였다. 적층구조의 면내크기가 1μm^2 보다 작을 때, 30 K 의 전류-전압특성에서 임계전류밀도 (*Jc*)가 크게 줄어드는 것이 발견되었다. 본 논문에서는 *Jc* 의 줄어듬 (suppression)에 대한 여러 가지 가능한 메커니즘에 대하여 논의하였고, 양자페이즈요동 (fluctuations)의 가능성의 관점에서 분석되었다.

본 논문에서는 Bi-2212 수염상단결정의 30 K 에서의 양자요동에 관하여 처음으로 보고 하였다. *a*-축배향 $YBa_2Cu_3O_7$ 박막은 샌드위치접합의 응용에

주로 사용되는 *c*-축 박막보다 코히어런스길이가 길기 때문에 소자응용에 있어서 보다 많은 가능성을 가지고 있음으로, *a*-축배향 초전도박막에 교차적으로 성장되는 *a*-축배향 에피탁셜 절연박막 혹은 일반금속 장벽층을 성장하는 것은 중요한 연구 목표중의 하나이다. 이러한 관점에서, 본 연구에서는 $YBa_2Cu_3O_7$ 와 $PrBa_2Cu_3O_7$ (Y123/Pr123)가 교차적으로 구성되는 다층의 서브마이크론 적층구조를 제작하고 연구를 수행하였다. 제작한 적층구조의 크기는 약 300 nm × 200 nm 이고 높이는 약 200 nm 이며, 임계온도는 84 K 이고, 30 K 에서 0.12 mA 의 임계전류를 나타내었다. 이 제작된 접합에서는 외부의 여러 가지 크기의 고주파파워에 따른 임계전류의 억압을 관찰하였다.

고주파 출력을 증가시킴에 따라 초전도 상태는 억제되고, 임계전류가 줄어드는 것을 발견하였지만, 전류-전압 특성에서 외부 고주파조사에 따른 교류조셉슨효과에 의한 샤피로스텝은 관찰 할 수 없었다. 또한. 집속이온빔 가공기술을 이용하여 두 개의 접합과 하나의 홀로 구성되는 초전도 양자간섭계(SQUID)형상의 소자를 제작하였으며, 고주파유기 전압스텝을 *I*-*V* 특성상에서 관찰하였다.

초전도전류는 마이크로출력의 증가에 따라 저항성을 가지게 되고, *Jc* 는 마이크로출력의 증가시킴에 따라 억제되었다. 관찰된 전압스텝의 파워의존성은 고주파파워에 따른 많은 수의 조셉슨접합이 볼텍스플로 (vortices-flow)현상에 기여함을 보여준다. 제작된 접합의 초전도체-반도체-초전도체 (S-S'-S)와 같이 거동하는 조셉슨접합전류의존성은 Ambegaokar-Baratoff 이론에 근거하여 근사함을 확인하였다.

CONTENTS

LIST OF FIGURES

LIST OF TABLES

1. INTRODUCTION

1.1 Introduction

The phenomenon of superconductivity was discovered in 1911 by a Dutch physicist H. Kamerlingh Onnes and his assistant Gilles Holst in Leiden. They found that *dc* resistivity of mercury suddenly drops to zero below 4.2 K, as shown in figure 1.1. The search for new superconducting materials led to a slow increase in the highest known transition temperature T_c over the decades, reaching a plateau at 23 K with the discovery of superconductivity of Nb_3Ge by Gavaler [1] in 1973. After 13 years, the discovery in 1986 of superconductivity at $\approx$ 35 K in "LBCO"(LaBaCuO phase) by Bednorz and Muller [2, 3] which opened the door for higher transition temperature superconductors and they were awarded Noble prize in 1987. This discovery was surprising and excited because it revealed that the oxides formed an unsuspected new class of superconducting materials with great potential other than large increase in T_c. Quickly the $T_c \approx 90$ K reached with the discovery of RE123 (RE is rare earth elements) class of material [4, 5, 6]. The achievement for more higher T_c were found in BiSCCO system [7] and TBCCO system [8]. In all these copper oxide planes form a common structural element, which is through to dominate the superconducting properties. Depending on the choice of stoichiometry, the crystallographic unit cell contains varying number of CuO_2 planes.

1.2 Josephson Junction

1.2.1 The Josephson effect

A tunnel junction consists of two strips of conducting materials separated by an insulator where the insulator is so thin that electrons can tunnel through it. A Josephson effect

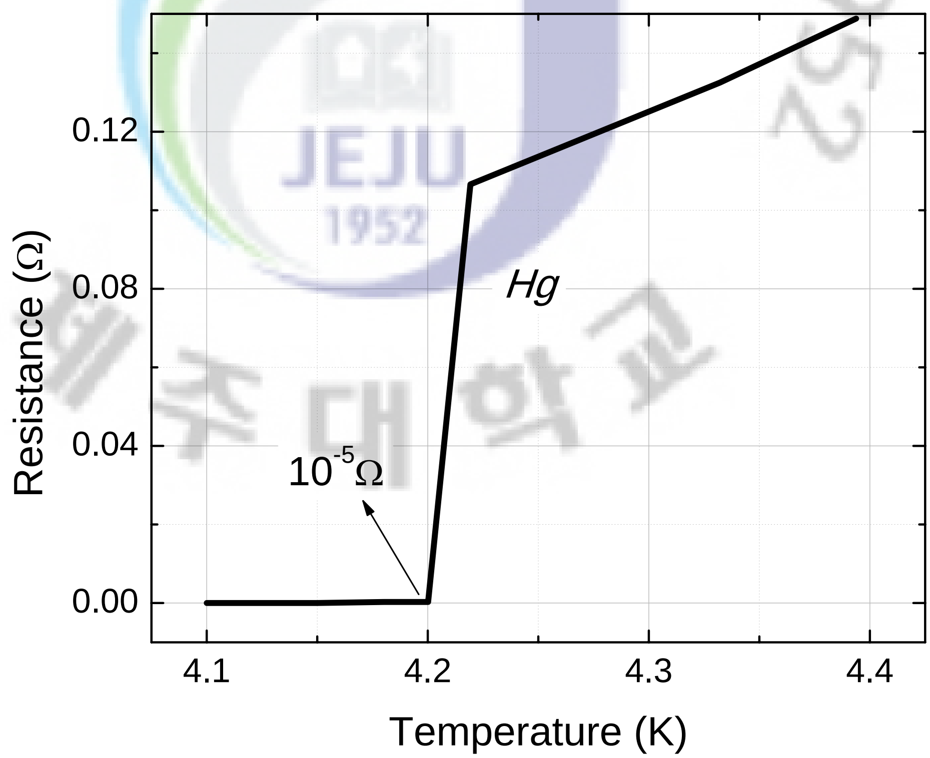

Fig. 1.1: The superconducting behavior observed in mercury by Gilles Holst and H. Kamerlingh Onnes in 1911, showing for the first time the transition from the resistive state to the superconducting state.

[9] is a phenomenon when these two strips are superconducting in the tunnel junction and the Cooper pairs can tunnel through the insulating barrier. Josephson predicted the occurrence of some unusual phenomenon in this situation a tunneling current at zero bias voltage. Shortly, this was observed experimentally and lead to the Nobel Prize to Josephson and Anderson. The structures which exhibits these phenomenon are known as Josephson junctions or weak links like Ref [10, 11, 12, 13, 14, 15]. Apart from these structures, in high T_c copper oxide materials (e.g. Bi-2212) *intrinsic* Josephson junctions (IJJs)tunneling occurs in the c-axis direction [16]. Figure 1.2 shows the schematic of different type of Josephson junctions. The insulating barrier is so thin that Cooper pairs can tunnel through it.

In Josephson junction, the thin insulating layer allows the overlap of wave functions in two superconductors, resulting in the Cooper-pair tunneling. The current density (**j**) in a superconductor can be described using the second Ginzburg-Landau (G-L) equation [17],

$$\mathbf{j} = -\frac{1}{2e\mu_\circ\lambda^2}(\hbar\nabla\theta + 2e\mathbf{A}) \tag{1.1}$$

where λ is the London penetration depth and **A** is the vector potential. Equation 1.1 shows that the *dc* current in superconductor can be determined by the phase difference in absence of magnetic field. If a junction is biased with current and the Cooper pairs tunnel through the tunneling barrier, the phase difference between two superconductors is defined by $\phi = \theta_1 - \theta_2$. This super current is defined by the *dc* Josephson effect as

$$I_J = I_c \sin_\phi \tag{1.2}$$

where I_c is the Josephson critical current. However the phase difference in an external magnetic field should be invariant under a gauge transformation of the vector and scalar potential. So the value of ϕ can be defined as

$$\phi = \theta_1 - \theta_2 + \frac{2e}{\hbar}\int_2^1 \mathbf{A}.d\mathbf{l} \tag{1.3}$$

When the junction is voltage biased, ϕ temporally oscillate according to the *ac* Joseph-

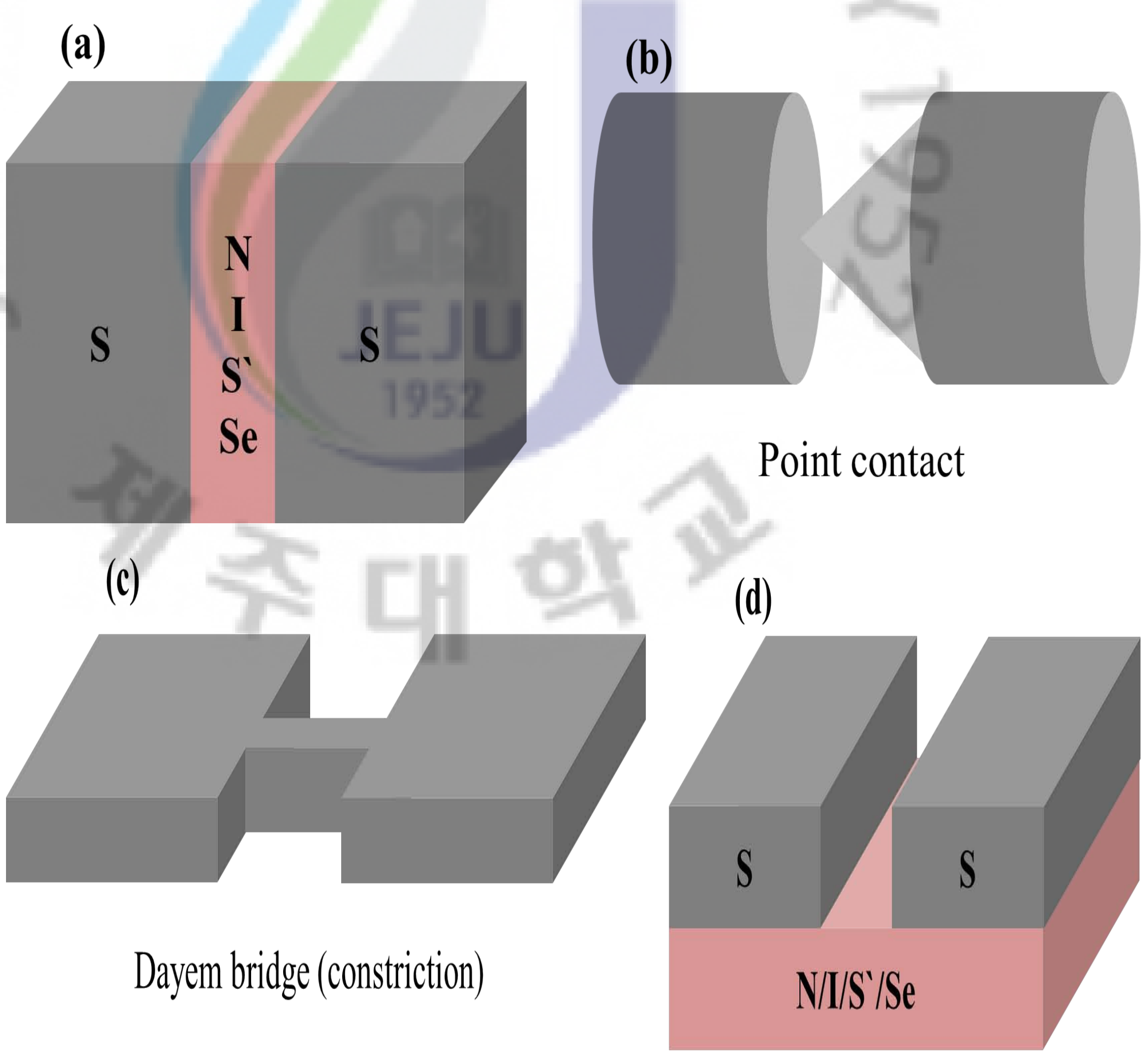

Fig. 1.2: The Schematic of different type of Josephson junctions. Where S stands for superconductor, S′ for a superconductor above T_c, N for normal metal, Se for semiconductor, and I for an insulator.

son effect,

$$\partial_t \phi = \frac{2e}{\hbar} V = \frac{2\pi}{\Phi_\circ} V \tag{1.4}$$

$$\frac{2e}{h} \approx 483.6\ GHz/mV (or\ \Phi_\circ\ is\ 2.067 \times^{-15}\ wb) \tag{1.5}$$

where $\Phi_\circ = h/2e$ is the flux quantum. The equation 1.2 and 1.4 predict that the oscillating current exists across the junction with the frequency $f_J = V/\Phi_\circ$ when a finite voltage V is biased across the junction. This properties provide the possibility of applications to the voltage standard devices and the high frequency devices such as oscillators and mixers [18].

1.3 The Quantum Regime

The Josephson junction shows a unique phenomenon when the size is sufficiently small so that the charge of a single electron matters. In quantum regime, the quantum conjugate properties of phase and number play an important role. This opens a wide path for new applications of Josephson junctions in quantum regime [19, 20, 21].

1.3.1 The Coulomb charging energy

The Coulomb charging energy (E_c) of a single electron, $E_c = e^2/2C$ should be considerably larger than thermal energy (K_BT), in order to eliminate thermal fluctuations.

1.3.2 Tunneling resistance

The tunneling resistance must exceed the quantum resistance $R_Q = h/4e^2 = \Phi_\circ/2e \approx 6.45\ k\Omega$ to avoid the effect being washed out by *quantum fluctuations* in the particle number.

1.3.3 The Josephson energy

The Josephson energy (E_J) is given by,

$$E_J = \frac{\Phi_\circ}{2\pi} I_c \tag{1.6}$$

where $\Phi_\circ = h/2e$ is the flux quantum and I_c is the superconducting critical current.The critical current is given by the Ambegaokar-Baratoff relation [22, 23],

$$I_c = \frac{\pi\Delta(T)}{2eR_N} \tanh \frac{\Delta(T)}{2k_B T} \tag{1.7}$$

where R_N is normal state resistance of the junction and Δ is the superconducting gap.

1.4 The RCSJ Model

In the resistively and capacitively shunted junction (RCSJ) model, an external bias current flows through three channels connected in parallel. The schematic of the model is shown in figure 1.3. In which the total current through the junction is the sum of the three components: the dissipation current I_R due to the effective ohmic resistance R, the displacement current I_D due to the effective capacitance C, and the super current I_J by the Josephson pair tunneling as,

$$I = I_R + I_J + I_D = V/R + I_c \sin\phi + CdV/dt \tag{1.8}$$

Substituting the value of V in the term of ϕ using equation 1.4 which gives the second order differential equation

$$I = \frac{\hbar}{2e}\left(C\partial_{tt}\phi + \frac{1}{R}\partial_t\phi\right) + I_c \sin_\phi \tag{1.9}$$

further,

$$\left(\frac{\hbar}{2e}\right)^2 \left(C\partial_{tt}\phi + \frac{1}{R}\partial_t\phi\right) + \partial_\phi U(\phi) = 0 \tag{1.10}$$

where $U(\phi)$ is the potential energy given by,

$$U(\phi) = -E_J\left(\cos\phi + \frac{I}{I_c}\phi\right) \tag{1.11}$$

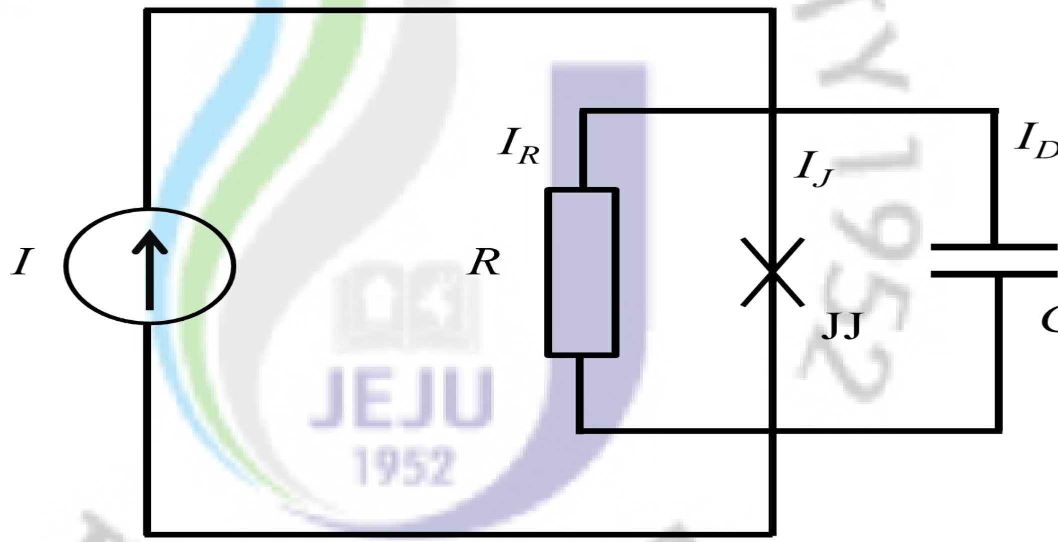

Fig. 1.3: In the RCSJ model, the junction consists of three elements, an ideal junction, a capacitor, and a linear resistor. In this case, the junctions is driven by a *dc* current source.

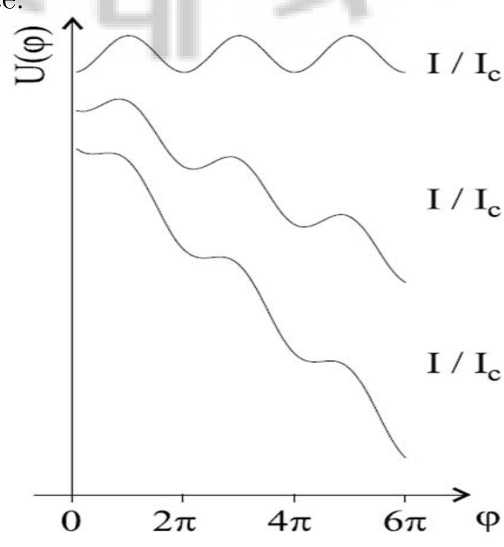

Fig. 1.4: The RCSJ model has a mechanical analog in the form of a particle in a washboard where the potential landscape changes with the slope of the board, given by I/I_c.

Here, $E_J = \hbar I_c/2e$ is the Josephson energy. A mechanical analog can be described by equations 1.10 and 1.11, a phase with mass m = C$(\hbar/2e)^2$ and an ohmic damping constant $1/RC$ moves along the ϕ axis in an effective tilted washboard potential U(ϕ) as shown in figure 1.4.

According to the washboard potential model, a particle is initially confined in the potential well at $\phi \approx \phi_\circ$ without a bias current. As we increase the bias current, the wash board potential is effictively tilted as shown in figure 1.4. Then a phase particle slides down the washboard, gaining an additional phase difference and a voltage drop occurs across the junction.

1.5 Intrinsic Josephson junction

Bi-2212 is a layered high-temperature superconductor which has highly anisotropic electric characteristics in the normal and superconducting states. Bi-2212 crystals are a closely packed naturally grown Josephson junctions as shown in figure 1.5. The CuO_2 bilayer plane (0.3 nm in thickness) and the BiO-SrO layer (1.2 nm in thickness) act as the superconducting electrode and the tunneling barrier, respectively. The layered crystal forms a three dimensional superconductors by a weak Josephson coupling between the superconducting layers and referred as *intrinsic Josephson junctions* (IJJs). The evidence for the existence of the Josephson junctions effect in the Bi-2212 intrinsic junctions has been revealed in the observation of the Fraunhofer diffraction pattern, Shapiro steps, Fiske steps, etc [24, 25, 26, 27].

1.6 SSeS type Josephson junction

A Josephson junction consists of semi conducting layer as a tunneling layer and sandwiched by superconducting layer referred as superconducting-semi conducting-superconducting (SSeS) Josephson junctions. A part of the thesis is based on SSeS type Josephson junction in which a-axis oriented $PrBa_2Cu_3O_7$ (Pr123) and a-axis oriented $YBa_2Cu_3O_7$ (Y123) act as a semi conducting layer and superconducting layer, respectively. The orientation of Y123 thin film can be controlled in any axis from a-axis to c-axis [28]. A-axis oriented thin films are potentially superior to c-axis films for sandwich-type junction applications be-

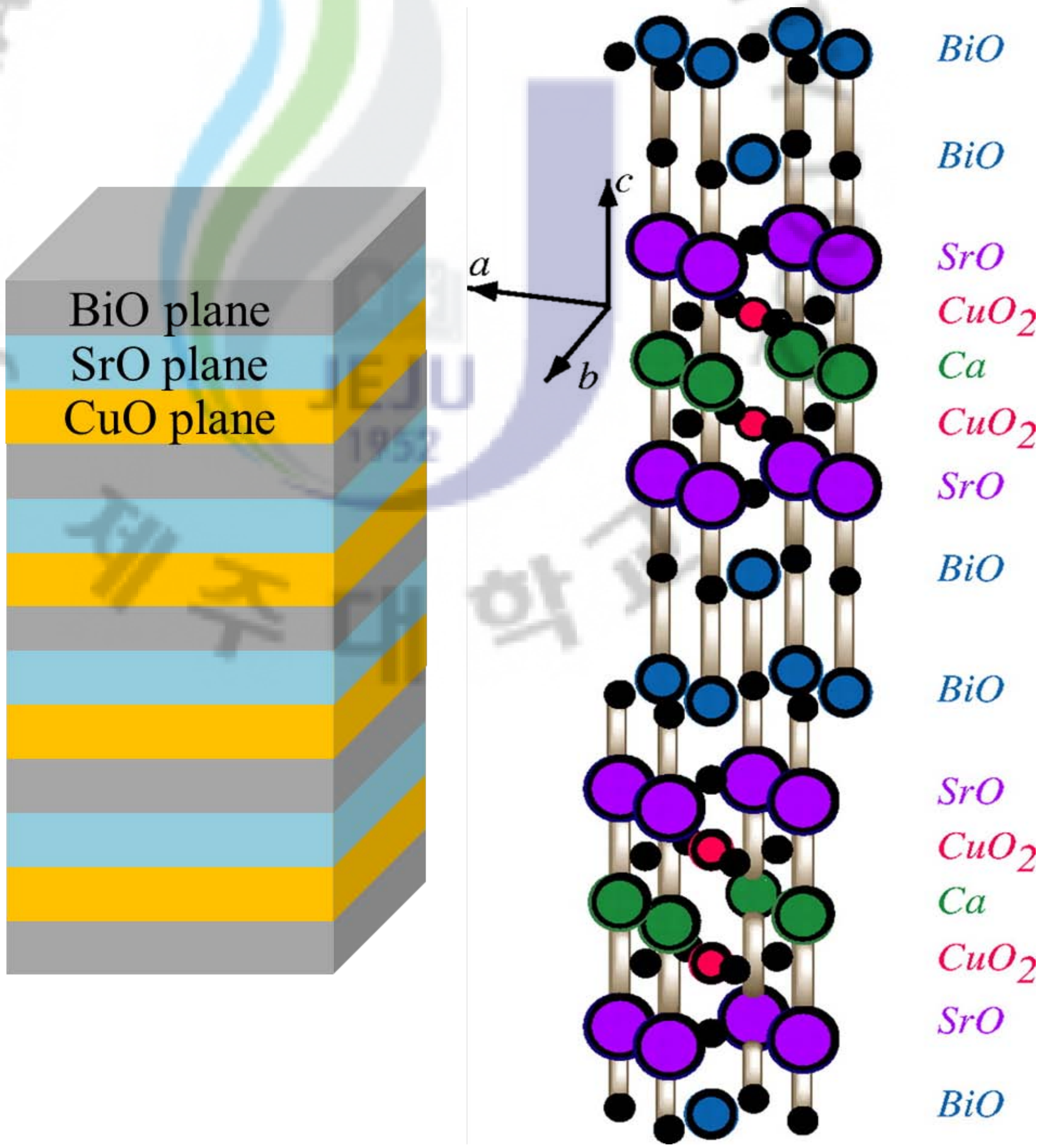

Fig. 1.5: Schematic of intrinsic Josephson junctions and the unit cell of Bi-2212 single crystal.

cause of the larger coherence length in a-axis direction [29]. Thus growth of thin epitaxial insulators or normal barriers on a-axis films, followed by another a-axis superconductor, is an important goal. The application of microwave irradiation on such multi layered thin film Josephson junctions (JJs) can be use in the quantum electronics devices [30]. Figure 1.6 shows a schematic of Y123/Pr123/Y123 Josephson junctions. The thin films are deposited on (100) $SrLaGaO_4$ (SLGO) substrates with buffer layer of Gd_2CuO_4(Gd214) by pulse laser deposition (PLD) technique. The red lines in the figure indicates the CuO planes.

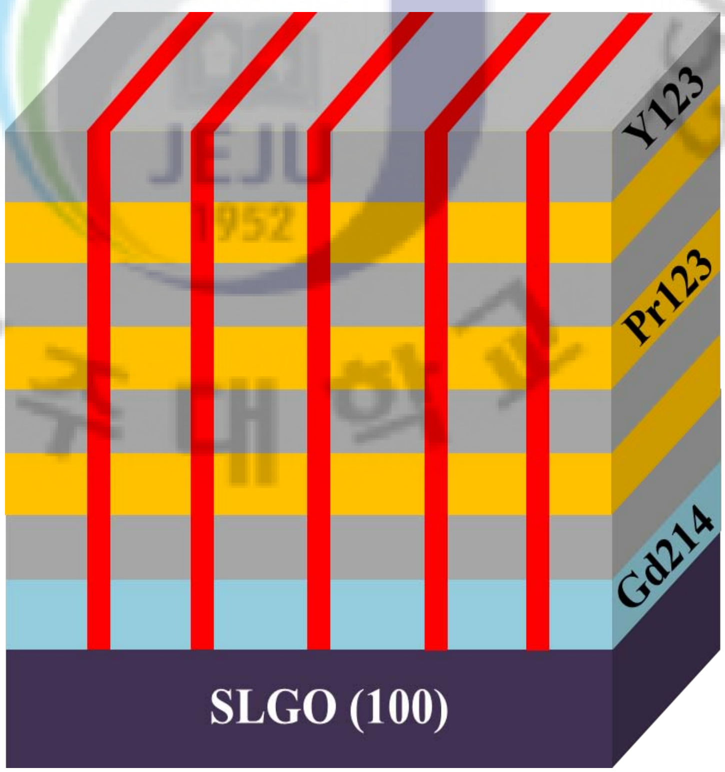

Fig. 1.6: Schematic of SSeS Josephson junctions and the red planes indicates the CuO planes in multylayered thin films.

1.7 Applications

Since the discovery of superconductor many potential applications are achieved. Table 1.1 is a summarized view in our knowledge based on superconductivity. A few of applications based on Josephson junction phenomenon are described in detail in following subsections.

Tab. 1.1: Various application of superconductivity

Concepts	Applications
R = 0 and high critical current density	Magnets for various application
	Passive microwave devices
	Interconnects in microelectronics
	Electrical energy transport by cables
Josephson tunneling	Microwave detectors and mixers
	In physical measurements (SQUIDs etc)
	Computers (fast logic and memory circuits)
	Plasma and space
High critical current at high critical magnetic field	Electrical power industry
	Plasma confinement (in high energy physics)
	In transport (levitation trains, MHD-propelled ships)
	Medicine (nuclear magnetic resonance tomography)

1.7.1 The Coulomb blockade

A Josephson junction or a tunnel junction has a wide scope for application based on Coulomb blocking phenomenon such as a voltage standard, single electron transistor, etc [19, 20, 21]. The Coulomb blockade refers to the modifications of the tunneling current-voltage characteristics which occur in the junctions with capacitance sufficiently small so that the Coulomb charging energy $E_c = e^2/2C$ of a *single* electron is large enough to play a major role.

Considering the electrostatic energy of an isolated capacitor C with charges Q (>0) and -Q on the two electrodes is $Q^2/2C$ or $CV^2/2$ where $V = Q/C$. Now if a electron tunnels from the negative electrode to the other one, the charge on the capacitor becomes $Q - |e|$, so that the energy of the capacitor becomes $(Q - |e|)^2/2C$. This represents an increase in system energy unless the initial charge $Q \geq |e|/2$, or equivalently, $V \geq |e|/2C$. Thus the electron transfer is energetically forbidden for voltages such that $|V| < |e|/2C$. This regime of zero tunnel current despite a finite voltage across the junction is an example of Coulomb blockade.

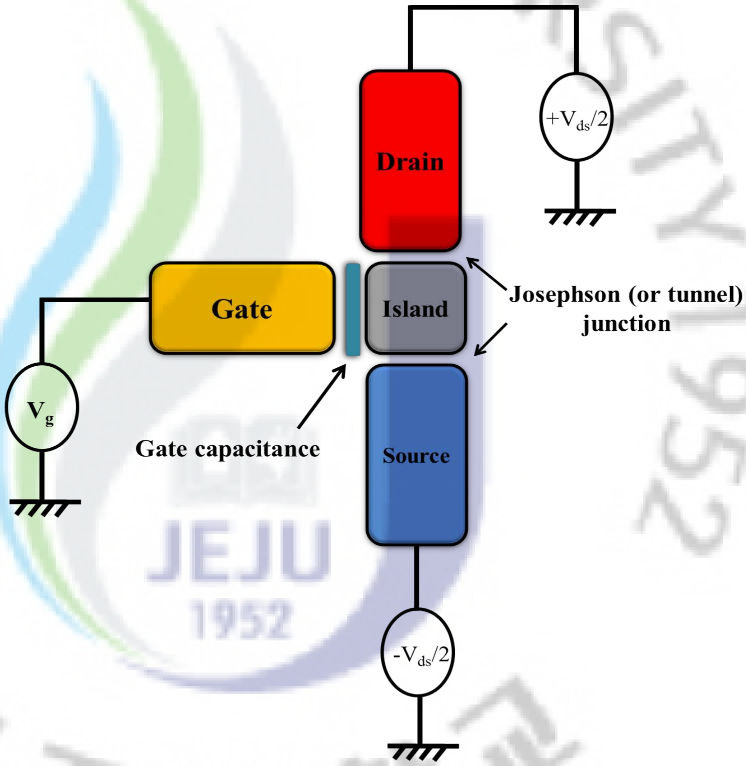

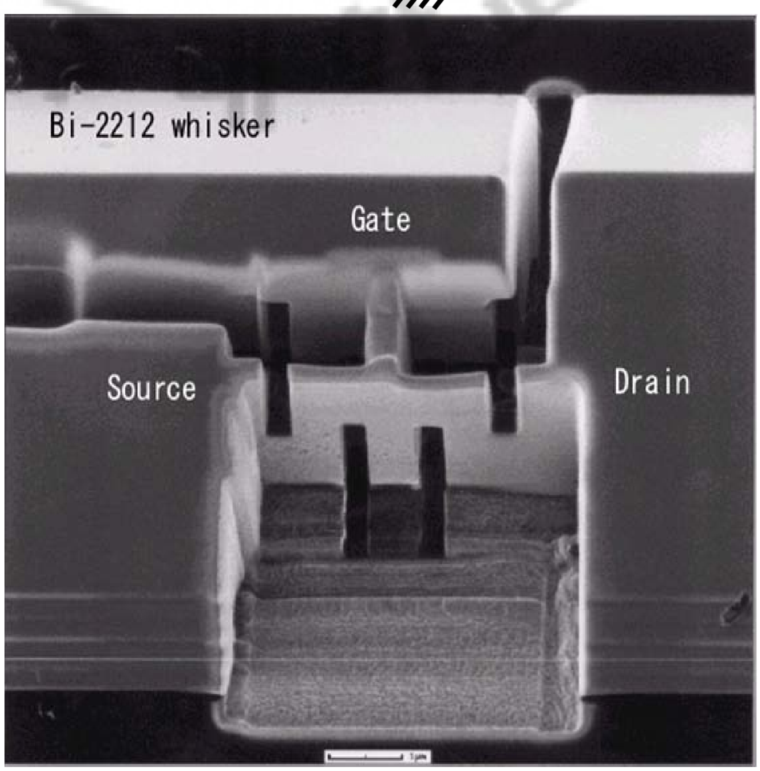

Fig. 1.7: The first image shows a schematic of SET and second image shows a fabricated device in Bi-2212 single crystal whisker taken from ref [31].

Single Electron Transistor (SET)

The simplest device in which the effect of Coulomb blockade can be observed is known as the single electron transistor (SET). It consists of two Josephson junctions or tunnel junctions sharing one common electrode with a low self-capacitance, known as the island. The electrical potential of the island can be tuned by a third electrode (the gate), capacitively coupled to the island. Figure 1.7 shows a schematic of SET along with a fabricated device in Bi-2212 single crystal whisker is referred from previous report [31].

1.7.2 Terahertz applications

The Josephson effect has always been focused by the researcher because of its wide application in science and technology. The Josephson effect provides a unique principle to excite high-frequency electromagnetic (EM) wave in the single junctions or in arrays. The Josephson junctions can be used as the terahertz (THz) oscillator because of large superconducting gap. Although the emission from a single junction is weak and many junctions can emit high enough power for different applications [32, 33, 34]. The solid-state THz radiation sources are useful for the application such as medicine, diagnostics, bio-science, ultrahigh-speed communication, environmental studies, security systems, and nondestructive and noninvasive sensing and imaging [35].

There are many studies have been done in high temperature layered superconductors. It has been challenging to synchronize all Josephson junctions in the stack. Various approaches for synchronizing the junctions have been studied such as applying a magnetic field to induce coherent Josephson vortex flow [36, 37, 38, 39, 40, 41] or putting the the device into a microwave cavity [42]. However the emitted power is in the range of pW only. Further a few of studies have shown a synchronized radiation of THz in the mesa of Bi-2212 of the power in range of μW. This synchronization was generated by a voltage biasing in c-axis in the absence of an external magnetic field. The EM emission takes place at the biasing voltage when the frequency determined by the *ac* Josephson relation equals to the fundamental cavity mode and corresponds to a half-wavelength of the plasma in the mesa. Synchronization of IJJs and mechanism behind the emission has given with coupling the cavity resonance with Josephson plasma frequency[43]. Wang et al. [43]

presented the cavity resonance can't be the only mechanism to synchronize the IJJs and THz radiation. The hot spot (a region above the transition temperature) formed within the mesa give rise to coherent THz emission.

1.8 Conclusions

The quantum devices using Josephson junction phenomenon has been demonstrated. The application is focused on single electron transistor and teraherz devices. The low capacitance devices is demonstrated in this thesis. A part of this thesis also concentrated on the teraherz irradiation on submicron devices. These devices are expected to be next generation devices for science and technology.

BIBLIOGRAPHY

[1] J. R. Gavaler, Appl. Phys. Lett. **23, 480** (1973).

[2] J.G. Bednorz and K. A. Muller, Z. Phys. **B64, 189** (1986).

[3] M. K. Wu et al, Phys Rev Lett **58, 908** (1987).

[4] S. Hikami et al, Jap J Appl Phys **26, L314** (1987).

[5] Z. X. Zhao et al., Kexue Tongbao **33, 661** (1987).

[6] H. Maeda et al, Jap J appl Phy **27, L209** (1988).

[7] Z. Z. Sheng and A. M. Hermann, Nature **232, 55** (1988).

[8] B. D. Josephson, Physics Letters **1, 251** (1962).

[9] J. E. Zimmerman and A.H. Silver, Phys. Lett **10, 47** (1964).

[10] P. W. Anderson and A. H. Dayem, Phys. Rev. Lett. **13, 195** (1964).

[11] J. Clarke, Proc. Roy. Soc. London A **308, 447** (1969).

[12] J. Clarke, Phys. Rev. B **4, 2963** (1971).

[13] C. H. Arrington and B. S. Deaver Appl. Phys. Lett. **26, 204** (1975).

[14] P. Chaudari, J. Mannhart, D. Dimos, C. C. Tsuei, J. Chai, M. M.Oprysko, and M. Scheuermann, Phys. Rev. Lett. **60, 16 1653** (1988).

[15] R. Kleiner, F. Steinmeyer, G. Kunkel, and P. Mueller, Phys. Rev. Lett. **68, 2394** (1992).

[16] M. Tinkham, *Introduction to Superconductivity 2nd edn (New York:McGraw-Hill)* (1996).

[17] A. Barone and G. Paterno, Physics and Applications of the Josephson Effects, John Wiley & Sons, New-York, (1982).

[18] J. Bylander, T. Duty, and P. Delsing, *Nature* **434 361** (2005).

[19] K.K. Likharev, *IBM J. Res. Develop.* **32 144** (1998).

[20] A. Aassime, P. Delsing, and T. Claeson, *Nanotechnology* **12 96** (2001).

[21] V. Ambegaokar and A. Baratoff, Phys. Rev. Lett. **10, 486** (1963).

[22] V. Ambegaokar and A. Baratoff, Phys. Rev. Lett. **11, 104** (1963).

[23] Yu. I. Latyshev, J. E. Nevelskaya, and P. Monceau, Phys. Rev. Lett. **77, 932** (1996)

[24] Yong-Joo Doh, Jinhee Kim and Kyu-Tae Kim, and Hu-Jong Lee, Phys. Rev. B **61, R3834** (2000)

[25] H. B. Wang, P. H . Wu, and T. Yamashita, Phys. Rev. Lett. **87, 107002** (2001)

[26] V. M. Krasnov, N. Mros, A. Yurgens, and D. Winkler, Phys. Rev. B **59, 8463** (1999)

[27] Y. Shingai, M. Mukaida, K. Matsumo, Y. Yoshida, A. Ichinose, S. Horii, A. Saito, and S. Ohsima, Physica C **412, 1296** (2004).

[28] T. K. Worthington, W. J. Gallagher, and T. R. Dinger, Phys. Rev. Lett. **59, 1160** (1987).

[29] C. P.Foley and H. Hilgenkamp, Supercond. Sci. Technol. **22, 064001** (2009).

[30] S.-J. Kim and T. Yamashita, Jour. Appl. Phys. **89 7675** (2001).

[31] V. P. Koshelets and S. Shitov, Supercond. Sci. Technol. **13, R53** (2000).

[32] R. Kleiner et al., Phys. Rev. Lett. **68, 2394** (1992).

[33] A. A. Yurgens, Supercond. Sci. Technol. **13, R85** (2000).

[34] Y.-S. Lee, Principles of Terahertz Science and Technology Springer, New York, (2009).

[35] H. B. Wang et al., Appl. Phys. Lett. **89, 252506** (2006).

[36] M.-H. Bae, H.-J. Lee, and J.-H. Choi, Phys. Rev. Lett. **98, 027002** (2007).

[37] K. Kadowaki et al., Physica C **437-438, 111** (2006).

[38] A. Irie, Y. Hirai, and G. Oya, Appl. Phys. Lett. **72, 2159** (1998).

[39] V. M. Krasnov, N. Mros, A. Yurgens, and D. Winkler, Phys. Rev. B **59, 8463** (1999).

[40] S. M. Kim et al., Phys. Rev. B **72, 140504** (2005).

[41] S. Madsen, G. Fillatrella, and N. F. Pedersen, Eur. Phys. J. B **40, 209** (2004).

[42] L. Ozyuzer, A. E. Koshelev, C. Kurter, N. Gopalsami, Q. Li, M. Tachiki, K. Kadowaki, T. Yamamoto, H. Minami, H. Yamaguchi, T. Tachiki, K. E. Gray, W.-K. Kwok, and U. Welp, Science **318, 1291** (2007).

[43] H. B.Wang, S. Guenon, B. Gross, J. Yuan, Z. G. Jiang, Y.Y. Zhong, M. Grunzweig, A. Iishi, P. H.Wu, T. Hatano, D. Koelle, and R. Kleiner Phys. Rev. Lett. **105, 057002** (2010)

2. GROWTH OF BI-2212 SINGLE CRYSTAL WHISKERS

2.1 Introduction

Whiskers can be used in the fabrication of new electronic devices with the application of intrinsic Josephson junction effects and related phenomenon. Growth and characterization of high temperature superconducting single crystal whiskers have always been focused by researchers because of perfect crystalline structure and the ability to study in small cross sections (when width and thickness are less than the magnetic field penetration depth). There are three compounds in the Bi-family high temperature superconductors, differing in the type of planar CuO_2 layers; single-layered $Bi_2Sr_2CuO_{6+\delta}$ (Bi-2201) single crystal, double-layered $Bi_2Sr_2CaCu_2O_{8+\delta}$ (Bi-2212) single crystal, and triple-layered $Bi_2Sr_2Ca_2Cu_3O_{10+\delta}$ (Bi-2223) single crystal. The Bi-2212 single crystal has the one of the most stable state in this family [1, 2, 3, 4].

In Bi-2212 single crystal whisker, the conducting CuO_2 planes are separated by an insulating BiO-SrO layer. This layered phenomenon gives high anisotropy to Bi-2212 single crystal whiskers and a naturally grown superconductor-insulator-superconductor (SIS) intrinsic Josephson junction (IJJ). These junctions are attractive because the current - voltage (IV) property along the c-axis of the IJJs has anomalous nonlinear characteristics and a series of several hundred Josephson junctions can be easily obtained [5].

The various methods to grow the high-quality Bi-family single crystal whiskers has been suggested so far and most studies on Bi-2212 whisker done by melt quenched glassy precursors [6, 7, 8, 9, 10]. Nagao *et al.* reported the growth of Bi-2212 single-crystal whiskers by using tellurium (Te) -doped precursors [9]. This method shows more homogeneous and better qualities with different growth mechanisms and supposes that the Te element acts as a catalyst to enhance whisker growth. We have followed the same recipe to grow single crystal whiskers for the study in this thesis.

2.2 The growth process

The $Bi_2Sr_2CaCu_2O_{8+\delta}$ (Bi-2212) single crystal whiskers are grown by the solid state reaction method. A high-purity commercial powder of Bi_2O_3, $SrCO_3$, CuO and TeO_2 were used to grow a single crystal whisker. These powders were mixed in the proportional ratio of $Bi_2Sr_2Ca_2Cu_{2.5}Te_{0.5}O_x$. The mixture was ground and calcinated at 760 °C twice and at 820 °C once, in presence of air. Te was used to enhance whisker growth. The calcinated powder was pressed by a force 60 kN into a pellet. The pellet was 10 mm in diameter and 2≈3 mm in thickness. The pellet was kept in a pure alumina boat and annealed at 870 °C for 100 hours. Figure 2.1 shows the heat treatment process for single crystal whisker growth. Prior to that, the sample was heat treated at 880 °C for 15 min to promote partial melting as shown in the inset of figure 2.1. During the process we used an oxygen atmosphere with a constant flow of 150 mL/min. The whiskers were grown on the surface of pellet, being of various dimensions in length (0.5 to 3 mm), width (10 to 30 μm) and thickness (0.5 to 3 μm). Figure 2.2 shows the optical image of Bi-2223 single crystal whiskers have grown on a precursor pellet of $Bi_2Sr_2Ca_2Cu_{2.5}Te_{0.5}O_x$. The whiskers grow on the surface of pellet in every direction. These whiskers can be easily placed on the MgO substrate by a tweezer.

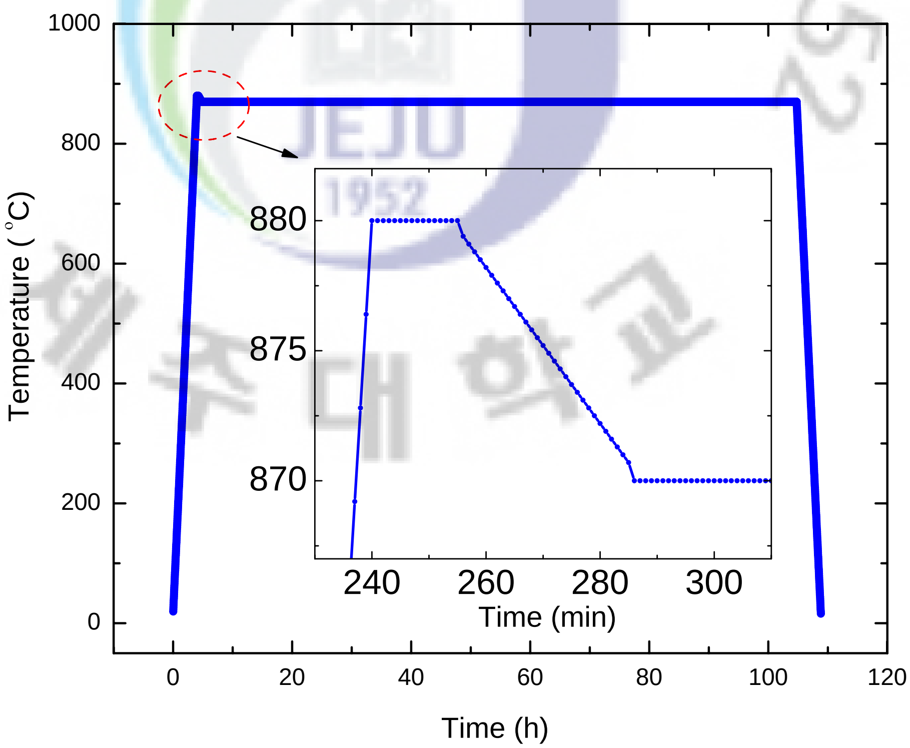

Fig. 2.1: The heat treatment process to grow Bi-2212 single crystal whiskers.

The magnified SEM image of a whisker indicates smooth surface of whisker. The smooth surface reflects good quality of the whisker see Figure 2.3. All four electrodes were prepared with silver paint on a whisker and attached on an MgO substrate. The sample was annealed at 450 °C for 5 min in presence of oxygen to reduce the contact resistance between whisker and silver paint.

2.3 Summary

The $Bi_2Sr_2CaCu_2O_{8+\delta}$ single crystals have been grown successfully using solid state reaction method. The SEM image showed a smooth surface of the whisker. These whiskers have been used in this thesis for submicron device fabrication and characterizations.

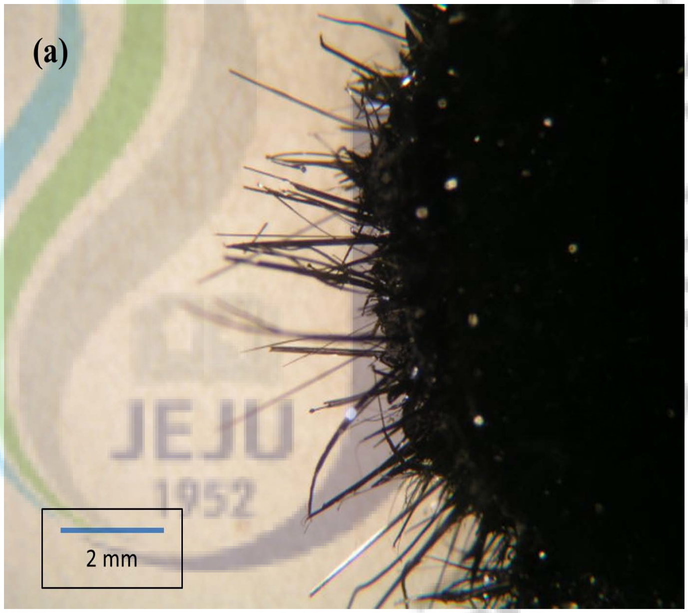

Fig. 2.2: A photograph of as grown single crystal whiskers on the precursor pellet.

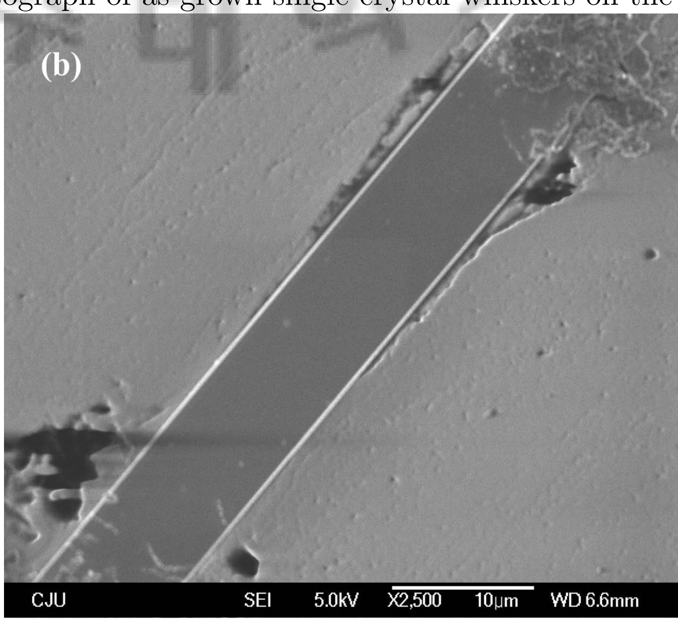

Fig. 2.3: A SEM image showing the smooth surface morphology of Bi-2212 single crystal whisker.

BIBLIOGRAPHY

[1] J. Appel and D. Fay, *Phys. Rev. B*, **41, 873** (1990).

[2] R. Kleiner, F. Steinmeyer, G. Kunkel, and P. Muller, *Phys. Rev. Lett.*, **68, 2394** (1992).

[3] G. Oya, N. Aoyama, A. Irie, S. Kishida, and H. Tokutaka, *Jap. J. Appl. Phys. Part 2*, **31, L829** (1992).

[4] P. Kleiner and P. Muller, *Phys. Rev. B*, **49, 1327** (1994).

[5] T. Yamashita and M. Tachiki, *Jap. J. Appl. Phys. Part 1*, **35, 4314** (1996).

[6] I. Matsubara, H. Tanigawa, T. Ogura, H. Yamashita, M. Kinoshita and T. Kawai, *Appl. Phys. Lett.* **58, 409** (1991).

[7] I. Matsubara, R. Funahashi, T. Ogara, H. Yamashita, K. Tsuru and T. Kawai, *J. Crystal Growth* **141, 131** (1994).

[8] Yu. I. Latyshev, I. G. Gorlova, A. M. Nikitina, V. U. Antokhina, S. G. Zybtsev, N. P. Kukhta and V. N. Timofeev, *Physica C* **216, 471** (1993).

[9] M. Nagao, M. Sato, H. Maeda, S-J. Kim and T. Yamashita, *Appl. Phys. Lett.* **79, 2612** (2001).

[10] S. Kishida, T. Hirao, S.-J. Kim and T. Yamashita, *Physica C* **195, 362** (2001).

3. FABRICATION TECHNIQUE

3.1 Introduction

A number of fabrication methods have been applied to develop high T_c superconducting devices [1, 2]. The fabrication of mesa structure in thin films and single crystal needs an intricate process and limits the minimum junction size due to required spaces for establishing electric contacts. The fabrication of tunneling devices of Josephson junctions in the layered high T_c superconductors are needed a special attention because of a perfect stacked structure with a very small lateral size compared with the Josephson penetration depth ($\lambda_J = \gamma_d$) [3, 4, 5], where $\gamma = \lambda_c/\lambda_{ab}$ is the London penetration depth anisotropy ratio and d is interlayer spacing [6].

The three dimensional focused ion beam (3D-FIB) etching method is a reliable and versatile technique for the fabrication of nanoscale Josephson junctions in single crystal whiskers. In FIB, a finely focused beam of gallium ions is used. As the beam rasters across the surface, an image of nanoscale resolution can be built up using secondary electrons when the FIB is operated at low beam currents. The FIB can also be operated at high beam currents for site specific sputtering or milling. The material is eroded like nanoscale sandblasting when the high-energy ion beam dwells on the sample.

3.2 The Focused Ion Beam

The FIB system has introduced in late 1980s and become an essential tool in the microelectronics industry. The principle of operation is similar to a Scanning Electron Microscope (SEM). The major difference is that in place of an electron source a gallium liquid metal source is used. This helps both imaging and milling of the sample. In addi-

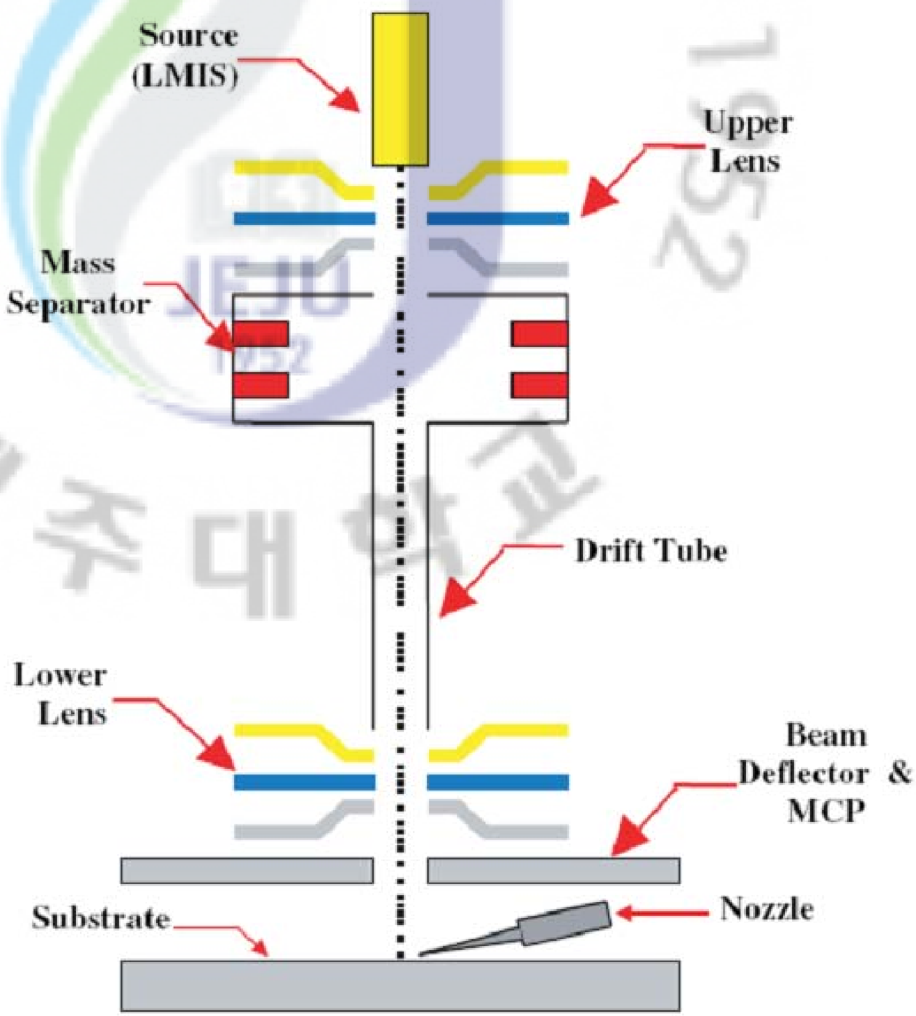

Fig. 3.1: The schematic of FIB operation.

Fig. 3.2: A photograph of FIB machine (SII NanoTechnology SMI2050) in Reseach Intruments Center (RIC).

tion, deposition of extra material can be achieved by ion beam-induced decomposition of an organometallic gas. Hence this versatile instrument allows faulty circuits to be both inspected and modified. Recent researches have exploited the ability of this instrument to create sub-micron scale features without resorting to complex and time-consuming techniques.

3.2.1 Operation of Focused Ion Beam

A liquid metal ion source (LMIS) is placed at top of the ion source chamber. A high vacuum ($= 6 \times 10^{-5}$ Pa) environment is maintained in the ion source chamber to avoid ion beam interference with gas molecules. An acceleration voltage is applied to ions to make ions pass through the ion column and move toward to the main chamber. The ions are focused to the fine ion beam by the aperture and electrostatic lenses in the ion column while passing through the ion column. The schematic of FIB machine is shown in figure 3.1.

To minimize the beam diameter it is necessary to use the highest beam voltage. The column voltage is 30 kV. The beam current (1 pA to 20 nA) is the rate at which ions strike the sample and is controlled by the variable aperture. A sample is fixed at the sample holder which is located in the main chamber (base pressure 5×10^{-4} Pa). When ion beam is irradiated, the secondary electron and the secondary ions are generated from the specimen surface. The secondary electrons or ions are converted into the electric signals and the two dimensional distribution of these signals is displayed as a microscope image. The atoms of the surface materials are expelled when ion beam is irradiated to the specimen. This phenomenon is used for etching to remove materials from the sample. When the irradiating ions beams while spraying a specific compound gas on the specimen surface, the solid elements of gas are adhered to the specimen surface and accumulated. This phenomenon is used for deposition of the material to the specimen surface.

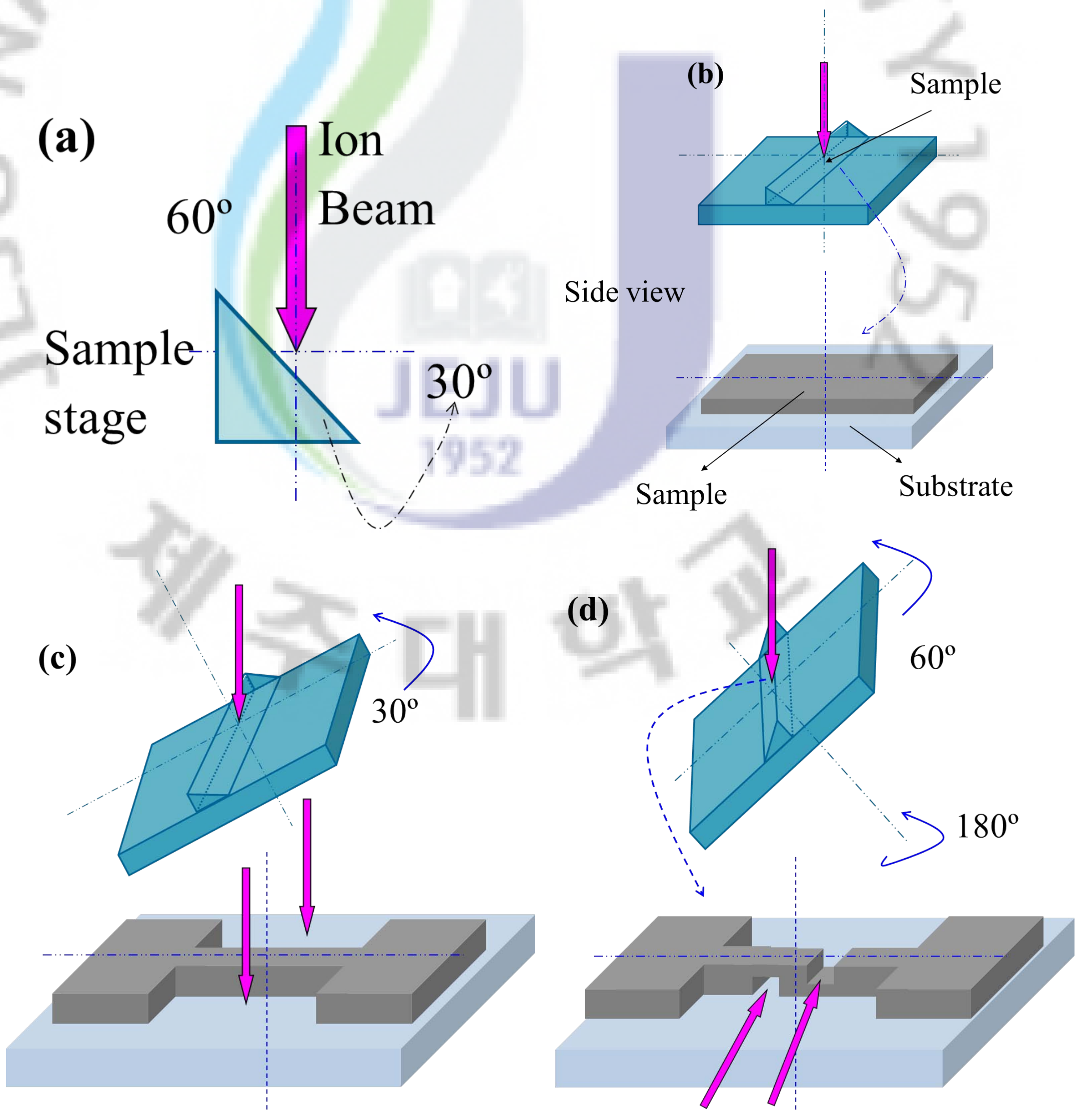

Fig. 3.3: The steps of fabrication process of Josephson junctions by FIB. (a) The inclined sample stage where we mount a sample. (b) A side view of as mounted sample on sample stage. (c) The first etching process to mill junctions in-plane area. (d) The final etching in two grooves.

3.3 Fabrication of Josephson junctions

In our laboratory the FIB machine (SII NanoTechnology SMI2050) can be used for etching as well as deposition of the materials. A picture of FIB machine is shown in figure 3.2. The FIB machine has a freedom of tilting and rotating the sample stage up to 60° and 360° respectively. A sample stage that itself inclined by 60° with respect to the direction of the ion beam is used for 3-D milling. The detailed fabrication process is shown in figure 3.3.

In the first step we milled sample in bridge pattern from the top direction. As shown in figure 3.3 (c), we tilted the sample stage by 30° so that the in-plane of sample was set to be perpendicular to the ion beam and the sample was milled in bridge pattern with desired junction area.

We turned sample stage back to the initial orientation and rotated it by 180° so that the inclined plane was set to be 60° with respect to the ion beam. We then tilted the sample stage by 60° so that the thickness of the sample was set to be perpendicular to the ion beam and two grooves of similar depths were etched the whole length and the distance between grooves was set according to the required junction size [7].

3.4 Summary

The fabrication process used to fabricate intrinsic Josephson junctions in $Bi_2Sr_2CaCu_2O_{8+\delta}$ (Bi-2212) single crystal whiskers is discussed in detail. We have achieved in-plane area down to 0.16 μm^2 for $Bi_2Sr_2CaCu_2O_{8+\delta}$ (Bi-2212) single crystal whiskers. We have also fabricated the Josephson junctions of a-axis oriented $YBa_2Cu_3O_7/PrBa_2Cu_3O_7$ (Y123/Pr123) multi layered thin films. In the case of Y123/Pr123 we have achieved in-plane area down to 200 nm × 300 nm. The results in this thesis shows that the submicron Josephson junction devices have been fabricated successfully using three dimensional focused ion beam milling technique.

BIBLIOGRAPHY

[1] L. R. Harriott, P. A. Polakos, and C. E. Rice, *Appl. Phys. Lett.* **55, 495** (1989).

[2] Q. Y. Ma, A. Wong, P. Dosanjh, J. F. Carolan, and W. N. Hardy, *Appl. Phys. Lett.* **65, 240** (1994).

[3] F. X. Regi, J. Schneck, J. F. Palmier, and H. Savary, *J. Appl. Phys.* **76, 4426** (1994).

[4] Yu. I. Latyshev, J. E. Nevelskaya, Physica C **235-240** 2991 1994.

[5] A. Yurgens1, D. Winkler1, T. Claeson1, and N. V. Zavaritsky, *Appl. Phys. Lett.* **70, 1760** (1997).

[6] L. N. Bulaevskii, J. R. Clem, L. I. Glazman, *Phys. Rev. B* **46, 350** (1992).

[7] S.-J. Kim, Yu. I. Latyshev, and T. Yamashita, *Supercond. Sci. Technol.* **12 729** (1999).

4. INTRINSIC JOSEPHSON JUNCTIONS STACK OF BI-2212

4.1 Introduction

Since the discovery of Bi-based high-T_c superconductors, much effort has been given to grow single crystal. Single crystal whiskers are always be in focused due to perfect crystallinity and unique properties in an ultra small sizes. In Bi-based single crystal whisker, the conducting CuO_2 planes are separated by insulating BiO-SrO layer [1]. This layered phenomenon gives high anisotropy to Bi-based single crystal whisker. Bi-based single crystal whisker is a naturally grown intrinsic Josephson junctions (IJJs). These junctions are attractive because the anomalous nonlinear current-voltage (I-V) characteristics along the c-axis and a series of several hundred Josephson junctions can be easily obtained [2].

The junctions are considered to be a one-dimensional array of Josephson junctions in the stack. IJJs are attractive objects for studying the Josephson effect. There are three compounds in the Bi-family high temperature superconductors, differing in the type of planar CuO_2 layers; single-layered $Bi_2Sr_2CuO_{6+\delta}$ (Bi-2201) single crystal, double-layered $Bi_2Sr_2CaCu_2O_{8+\delta}$ (Bi-2212) single crystal, and triple-layered $Bi_2Sr_2Ca_2Cu_3O_{10+\delta}$ (Bi-2223) single crystal [3]. The compounds have transition temperature (T_c) about 20 K, 85 K, and 110 K for Bi-2201, Bi-2212, and Bi-2223, respectively. However Bi-2223 has highest T_c in this family but the phase is not stable and difficult to grow. In our study, we have used Bi-2212 single crystal whiskers which has stable phase and high T_c. Figure 4.1 shows the unit cell of Bi-2212 single crystal whisker. The conducting CuO layers are separated by insulating BiO-SrO layers. The characteristics of IJJs can be measured by

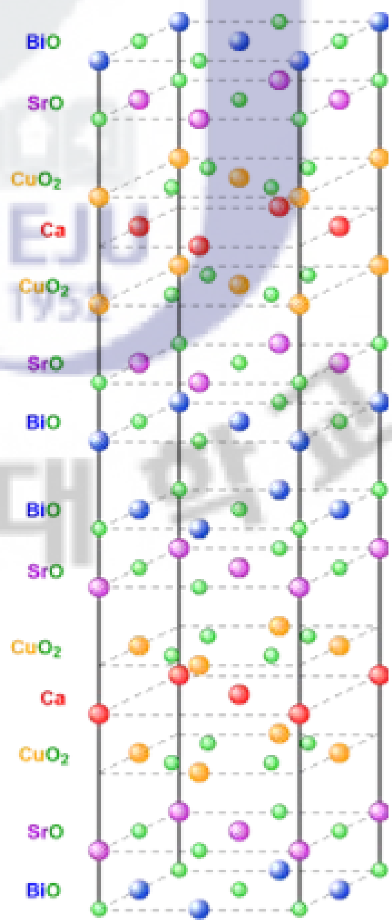

Fig. 4.1: The unit cell of Bi-2212 single crystal whisker.

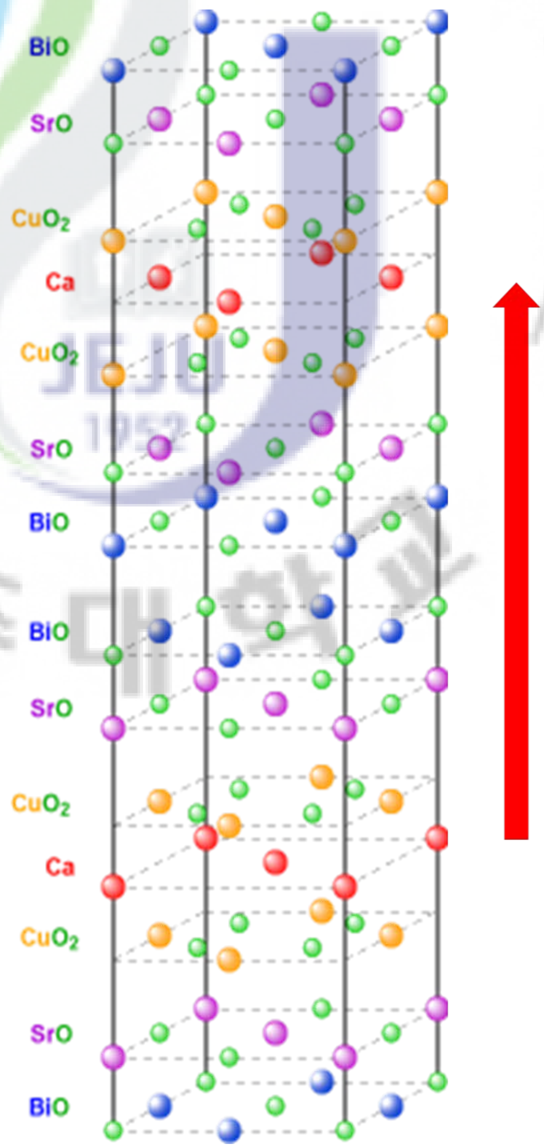

Fig. 4.2: The red arrow indicates the direction of current to measure the characteristics of IJJS in Bi-2212 single crystal whiskers.

flowing current in vertical direction as shown in figure 4.2. The red arrow in figure 4.2 shows the direction of current.

4.2 Experimental details

Bi-2212 single crystal whiskers used in this study were grown by solid state reaction method as described in chapter 2. A Bi-2212 whisker was placed on MgO substrate. The silver paint was used to make four electrodes for electrical characterization. To minimize contact resistance, the sample was annealed for 5 minutes at 450°C in presence of oxygen. The stacks were fabricated using three dimensional focused ion beam (3-D FIB) milling process. The stacks of various in-plane areas ($S \geq 1$) were fabricated using 3-D FIB machine (SII NanoTechnology SMI2050) in a Bi-2212 whisker, operating with a gallium ion beam of energy 30 keV and beam current from 1 pA to 20 nA. The detailed fabrication process is described elsewhere [4, 5]. Briefly in this process, the FIB machine has a freedom of tilting and rotating the sample stage up to 60° and 360° respectively. We used a sample stage that itself inclined by 60° with respect to the direction of the ion beam. We tilted the sample stage by 30° so that the ab-plane of sample was set to be perpendicular to the ion beam and the sample was milled along the ab-plane. We turned sample stage back to the initial orientation and rotated it by 180° so that the incline plane was set to be 60° with respect to the ion beam. We then tilted sample stage by 60° so that the c-axis of the sample was set to be perpendicular to the ion beam and the sample was milled along the c-axis. The Bi-2212 single crystal whisker was then etched the ab-plane. With the precise control in 3-D FIB fabrication process, we were able to achieve the height of stack about 100 nm. In this study, all whiskers were annealed before the 3-D FIB fabrication process to avoid Ga^+ ion contamination. All the measurement were done at 30 K. Table

Tab. 4.1: Parameters of Stacks of different in-plane area at 30 K

Stack	S (μm^2)	T_c (K)	N $\approx$	J_c (KA/cm^2)	C (fF)	Damping rate (μeV)	E_c (μeV)	N$\times E_c$ (meV)	E_J (meV)
J1	4	77	130	1.2	118	1	2.7	0.3	82.4
J2	3.5	80	100	0.86	103	0.4	3.1	0.3	72.1
J3	2.25	76	130	0.79	66	0.9	4.8	0.6	46.3
J4	1	78	130	1.1	29	1	10.8	1.4	20.6

4.1 describes the parameters of IJJs of the stacks with different in-plane areas at 30 K.

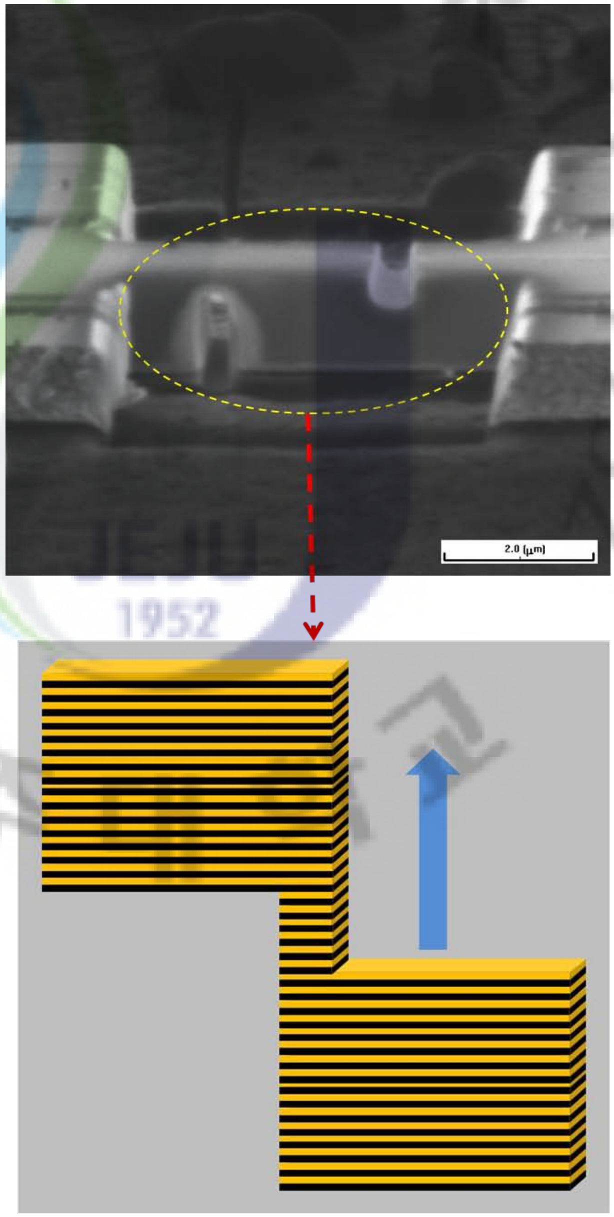

Fig. 4.3: FIB image of stack J1 (scale bar of 2 μm) and schematic of the IJJs configuration in the stack. The blue arrow indicates the direction of current flow which is along the IJJs.

Keithley 2182A nano voltmeter and Keithley 6221 AC & DC current source were used to measure resistance-temperature (R-T) characteristics and current-voltage (J-V) characteristics for different in-plane stacks using conventional four probe technique in current biasing mode. The low pass filters were used in signal line to reduce the external noise at room temperature.

4.3 Results and discussion

An FIB image of a stack J1 with the scale bar of 2 μm is shown in figure 4.3 along with the schematic of the stack. The dimensions of the stack J1 are 2 μm $\times$ 2 μm with height of 200 nm. The description of fabricated stacks of various S are summarized in Table 4.1. Conducting CuO planes are sandwiched by insulating BiO-SrO planes which work as IJJs [1]. These IJJs are arrange in series of an array in Bi-2212. The schematic of stack is also shown in figure 4.3. The spacing between these elementary IJJs is about 1.5 nm. The number of elementary IJJs ($N = z/1.5$) can be calculated from the height (z) of the stack [6, 7]. Therefore, the stack J1 has approximately 130 elementary IJJs. The approximate number of IJJs for various stack are shownn in table 4.1.

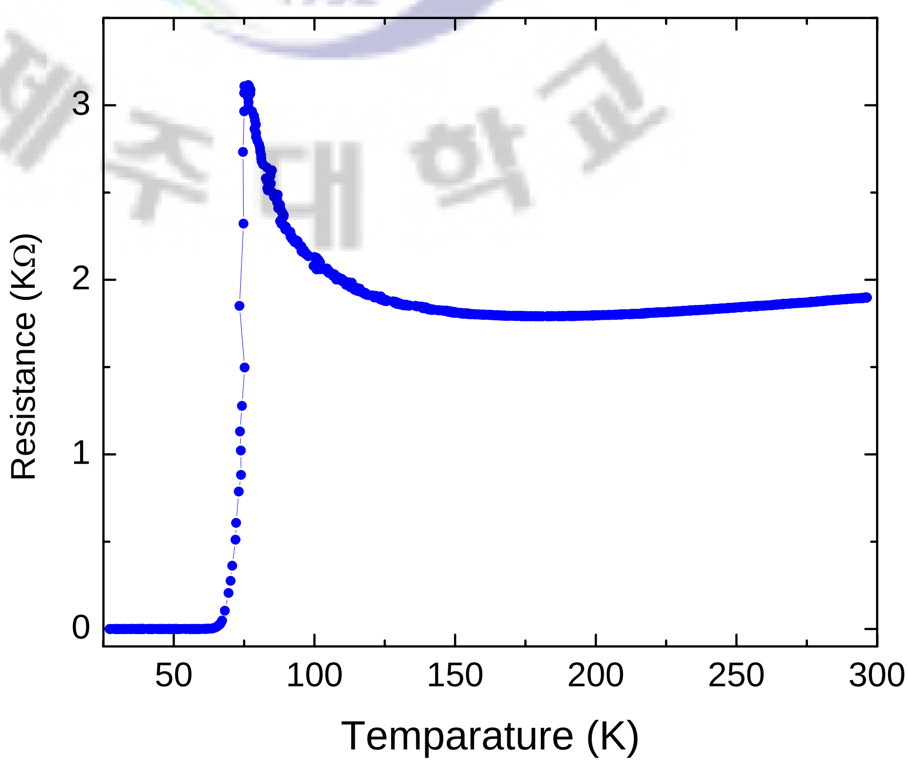

Fig. 4.4: The resistance vs temperature characteristics of stack J1.

Figure 4.4 depicts resistance vs temperature (R-T) characteristics along the c-axis, shows single phase superconducting transition (T_c) at about 77 K. The over all magnitude of c-axis resistance decreases monotonically and become about zero after. The nonlinearity of R-T characteristics before transition temperature can be described by the relation given by Yan et al [8] as equation 1.

$$R(T) = (a/T)e^{\Delta/T} + b/T + d \tag{4.1}$$

where a, b, and d are T independent parameters, while Δ represent pseudo gap

The charge transport between adjacent layers can be better described as tunneling between metallic layers, instead of the band conduction due to the high magnitude of c-axis resistance [8]. Ioffe et al.[9] have described para conductivity which contribute to increase resistance in c-axis above T_c. The single particle density of states at Fermi level has suppressed due to strong fluctuations into three-dimensional and reduces the c-axis current, also gives nonlinear resistance [9].

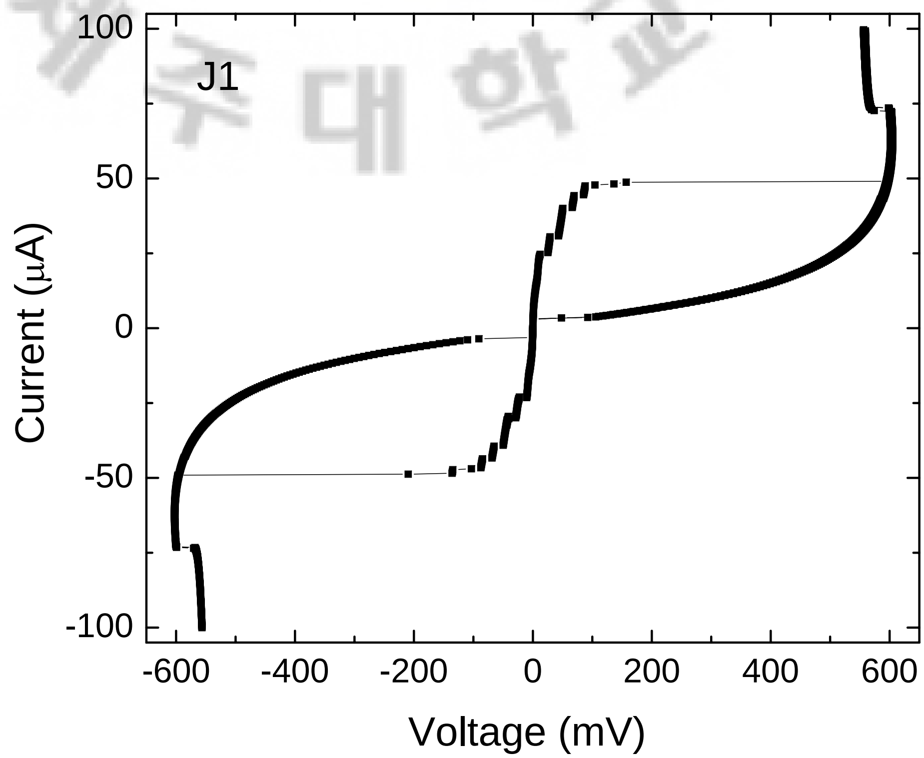

Fig. 4.5: The voltage vs current characteristics of stack J1 at 30 K.

Voltage dependence of current along the c-axis has been measured at 30 K and found to have nonlinear characteristic as shown in figure 4.5. We estimated critical current density (J_c) of stack J1 at 30 K abot 1.2×10^3 A/cm^2. The superconducting gap in I-V characteristics ($\approx$ 600 mV) shows a few hundred of elementary Josephson junctions in the stack, that are arranged in series as an array. The step structure near the super current branch indicates towards the tunneling from one IJJ to another IJJ and appeared as multi branch structure. To avoid the damage of the stack we have not flowed more current to observe resistive branch.

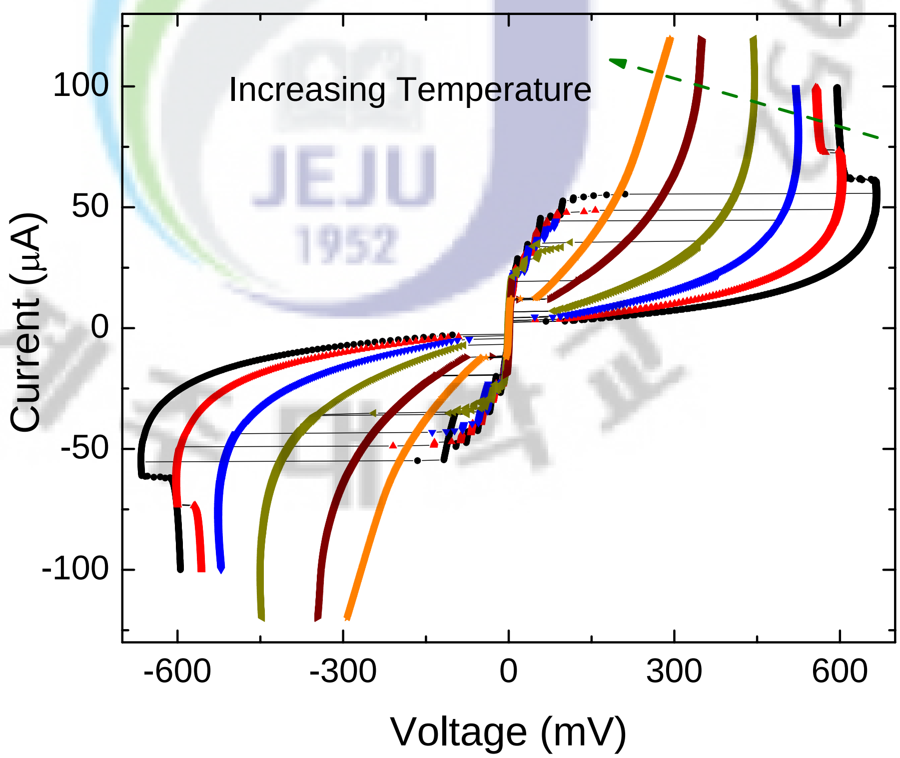

Fig. 4.6: The voltage vs current characteristics of stack J1 for various temperature 25 K, 30 K to 70 K in the interval of 10 K.

The I-V characteristics of the stack J1 were measured at different temperature and shown in figure 4.6. With increase in temperature, the critical current and the gap between the branches decreases. At high voltage at all temperatures, the I-V curve approaches to the straight line. This behavior is a consequence of usual tunneling theory. And above transition temperature it behave like Ohm's law (not shown here). The normal tunneling resistance is defined as the static resistance at high voltage where I-V curve sufficiently approaches the straight line and cross the origin. Figure 4.6 is also following the same phenomenon at high voltage biasing at any temperature 25 K, 30 K to 70 K with interval of 10 K. The maximum value of J_c about is observed at 25 K.

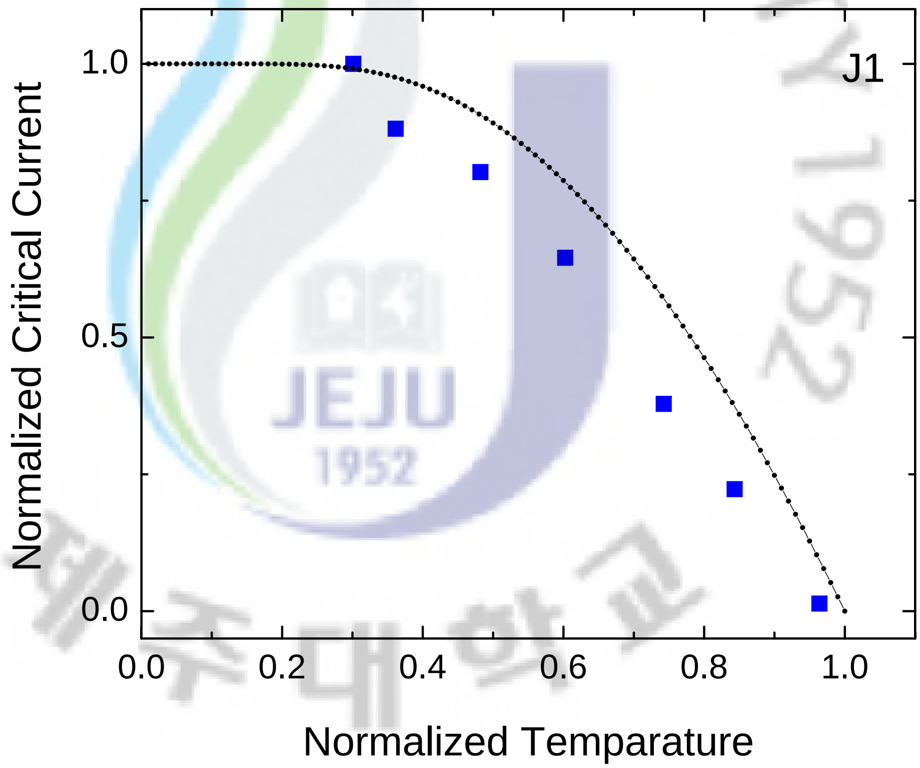

Fig. 4.7: Comparison of experimental data (solid square points) with the theoretical estimation of A-B theory for stack J1.

Further we have analyzed the type of IJJs in the stack. We plotted the temperature dependence of normalized critical current ($I_c/I_{c\ at\ 10K}$) in figure 4.7. The experimental data is compared with theoretical estimation of the Ambegaokar-Baratoff (A-B) theory [10]. The characteristics show superconducting-insulating-superconducting (SIS)-like Josephson junction which follows a good agreement with our experimental data. The results are same as reported before for SIS -like Josephson junctions. In figure 4.7 the blue solid squares are experimental data points and line is the theoretical estimation of A-B theory.

4.4 Conclusions

In conclusion, we have fabricated stack of intrinsic Josephson junctions of Bi-2212 whiskers of different in-plane areas. The transition temperature and critical current density are about 77 K and 1.2×10^3 A/cm^2 at 30 K is observed. The Ambegaokar-Baratoff relation indicates towards the superconducting-insulating-superconducting -like intrinsic Josephson junctions.

BIBLIOGRAPHY

[1] A. A. Levin, I. Y. Smolin, and F. Y. Shepelev *J. Phys. Condens.Matter* **6, 3539** (1994).

[2] T. Yamashita and M. Tachiki, *Jap. J. Appl. Phys. Part 1* **35, 4314** (1996).

[3] R. M. Hazen, C. T. Prewitt, R. J. Angel, N. L. Ross, L. W. Finger, C. G. Hadidiacos, D. R. Veblen, P. J. Heaney, P. H. Hor, R. L. Meng, Y. Y. Sun, Y. Q. Wang, Y. Y. Xue, Z. J. Huang, L. Gao, J. Bechtold, and C. W. Chu, *Phys. Rev. Lett.* **60, 1174** (1988).

[4] S.-J. Kim, Yu. I. Latyshev, and T. Yamashita, *Supercond. Sci. Technol.* **12 729** (1999).

[5] S. Saini, G. S. Kim, S. -J.Kim, *J. Supercond. Nov Magn* **23 811** (2010).

[6] Yu. I. Latyshev, S.-J. Kim, and T. Yamashita, *JETP Lett.* **69 84** (1999).

[7] P. A. Warburton, J. C. Fenton, M. Korsah, and C. R. M. Grovenor, *Supercond. Sci. Technol.* **19 S187** (2006).

[8] Y.F. Yan, P. Matl, J. M. Harris, and N.P. Ong, *Phys. Rev. B*, **52, R751** (1995).

[9] L.B. Ioffe, A.I. Larkin, A.A. Varlamov, and L. Yu, *Phys. Rev. B*, **47, 8936** (1993).

[10] V. Ambegaokar and A. Baratoff, *Phys. Rev. Lett.* **10, 486** (1963).

5. QUANTUM FLUCTUATION INDUCED SUPPRESSION OF CRITICAL CURRENT DENSITY IN SUBMICRON IJJS

The Cooper pair tunneling in the intrinsic Josephson junctions (IJJs) can be affected by quantum phase fluctuations when the resistance of a submicron stack is in the range of quantum resistance. To observe this quantum effect we have fabricated stacks of IJJs of various in-plane area from 4 μm^2 down to 0.16 μm^2 in $Bi_2Sr_2CaCu_2O_{8+\delta}$ single crystal whiskers using three-dimensional focused ion beam etching technique. For stacks of in-plane area less than 1 μm^2 a strong suppression in critical current density (J_c) is noticed in current-voltage characteristics at 30 K. The possible mechanisms in this suppression of J_c are discussed and the data analysis points to the quantum phase fluctuations as the most likely mechanism of this effect. We have achieved quantum fluctuations at 30 K first time ever reported for $Bi_2Sr_2CaCu_2O_{8+\delta}$ (Bi-2212) single crystal whisker.

5.1 Introduction

Intrinsic Josephson junctions (IJJs) are attractive objects for studying the Josephson effect. Depending on lateral size, large IJJs can be used as high frequency applications [1, 2]. The applications of submicron range IJJs can be related with Coulomb blockade and quantum phase fluctuations effect on Cooper pair tunneling [3, 4, 5]. The value of critical current density (J_c) can be highly affected by both, thermal or quantum phase fluctuations (QFs) [6]. Thermal fluctuations are important when the value of thermal energy ($k_B T$) is higher than charging energy (E_c). While QFs become important when: i) the resistance of junction approaches quantum resistance (R_Q=$h/4e^2$), ii) the value of

E_c is higher than $k_B T$ and comparable with Josephson energy (E_J) [7, 8, 9]. In the present work we found a suppression of J_c of submicron lateral sizes IJJs. The data analysis points to the QFs are the most likely mechanism of this effect.

To observe these QFs, the stacks are fabricated with different in-plane areas (S) from 4 μm^2 down to 0.16 μm^2 using three-dimensional focused ion beam (3-D FIB) etching technique in $Bi_2Sr_2CaCu_2O_{8+\delta}$ (Bi-2212) single crystal whisker. The value of J_c has suppressed when S approaches lower than 1 μm^2 which is the result of QFs in the phase.

5.2 Experimental details

Bi-2212 whiskers were grown by solid state reaction method using the high-purity powders of Bi_2O_3, $SrCO_3$, CuO and TeO_2. These powders were mixed in the proportional ratio of $Bi_2Sr_2Ca_2Cu_{2.5}Te_{0.5}O_x$. Further this powder was calcinated twice at 720 °C and once at 860 °C with intermediate grinding. The calcinated powder was pressed into a pellet of diameter 10 mm with a force of 60 kN. The pellet was heat treated at 880 °C for 100 h in an oxygen environment with the flow of 150 mL/min [10]. The whiskers of various dimensions in length (0.5 to 3 mm), width (10 to 30 μm) and thickness (0.5 to 3 μm) were found to grow from the surface of pellet.

A Bi-2212 whisker was mounted on MgO substrate. The silver paint was used to make four electrodes for electrical characterization. To minimize contact resistance, the sample was annealed at 450 °C for 5 minutes in presence of oxygen. The stacks of various in-plane areas (S) were fabricated using 3-D FIB machine (SII NanoTechnology SMI2050) in a Bi-2212 whisker, operating with a gallium ion beam of energy 30 keV and beam current from 1 pA to 20 nA. The detailed fabrication process is described elsewhere [11, 12]. Briefly in this process, the FIB machine has a freedom of tilting and rotating the sample stage up to 60° and 360° respectively. We used a sample stage that itself inclined by 60° with respect to the direction of the ion beam. We tilted the sample stage by 30° so that the *ab*-plane of sample was set to be perpendicular to the ion beam and the sample was milled along the *ab*-plane. We turned sample stage back to the initial orientation and rotated it by 180° so that the incline plane was set to be 60° with respect to the ion beam. We then tilted sample stage by 60° so that the *c*-axis of the sample was set to be perpendicular

Tab. 5.1: Parameters of IJJ of different in-plane area at 30 K

Stack	S (μm^2)	T_c (K)	N $\approx$	J_c (KA/cm^2)	C (fF)	Damping rate (μeV)	E_c (μeV)	N$\times E_c$ (meV)	E_J (meV)
J22	4	77	130	1.2	118	1	2.7	0.3	82.4
J33	3.5	80	100	0.86	103	0.4	3.1	0.3	72.1
J20	2.25	76	130	0.79	66	0.9	4.8	0.6	46.3
J19	1	78	130	1.1	29	1	10.8	1.4	20.6
J11	0.25	78	130	0.07	7	14	43.3	5.6	5.1
J24	0.16	77	130	0.03	4	2	67.8	8.8	3.3

to the ion beam and the sample was milled along the c-axis. The Bi-2212 single crystal whisker was then etched the ab-plane into the size of 0.4×0.4 μm^2 and the height of 200 nm along the c-axis. Table 5.1 describes the parameters of IJJs of the stacks with different in-plane areas at 30 K.

Keithley 2182A nano voltmeter and Keithley 6221 AC & DC current source were used to measure resistance-temperature (R-T) characteristics and current-voltage (J-V) characteristics for different in-plane stacks using conventional four probe technique in current biasing mode. The low pass filters were used in signal line to reduce the external noise at room temperature.

5.3 Results and discussion

An FIB image of the submicron stack J24 with the scale bar of 1 μm is shown in figure 5.1. The dimensions of the stack J24 are 0.4 μm $\times$ 0.4 μm with height of 200 nm. The description of fabricated stacks of various S are summarized in Table 5.1. Conducting CuO planes are sandwiched by insulating BiO-SrO planes which work as IJJs [13]. These IJJs are arrange in series of an array in Bi-2212. The schematic of stack is also shown in figure 5.1. The spacing between these elementary IJJs is about 1.5 nm. The number of elementary IJJs ($N = z/1.5$) can be calculated from the height (z) of the stack [14, 15]. Therefore, the stack J24 has approximately 130 elementary IJJs. The approximate number of IJJs for various stack in shown in Table 5.1.

In-plane area (S) dependence of J_c was measured at T = 30 K. The value of J_c is calculated from (critical current I_c)/S. Further the value of I_c is extracted by subtracting the quasiparticle current [8]. As shown in Table 5.1, for $S > 1$ μm^2, J_c is considerably

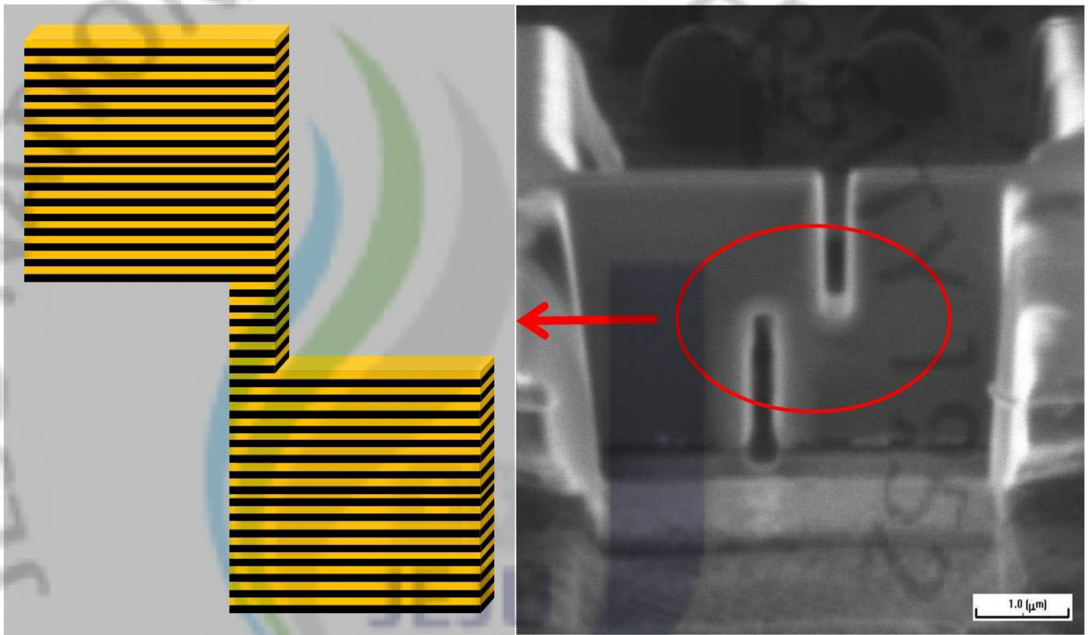

Fig. 5.1: FIB image of stack J24 (scale bar of 1 μm) and schematic of the IJJs configuration in submicron stack.

independent of S and approximately equal to 1×10^3 A/cm^2. This value of J_c is used as unfluctuated value of the critical current density ($J_{c\circ}$). The value of $J_{c\circ}$ is consistent with the theoretical value of J_c at $T = 0$ K ($J_c(0) = c\Phi_\circ/8\pi^2 s\lambda_c^2$) about 3×10^3 A/cm^2, which is considered to be fluctuation free, where $\Phi_\circ$ is flux quantum, $\gamma = \lambda_c/\lambda_{ab} \approx 1300, \lambda_{ab} = 0.3\ \mu m$ [14]. However for the submicron stacks, J_c is suppressed.

Figure 5.2 shows a comparison of J-V characteristics for big stack J22 and submicron stack J11 at 30 K. The value of J_c at 30 K is calculated about 1.2 kA/cm^2 and 0.07 kA /cm^2 for stack J22 and J11, respectively. A strong suppression of J_c of stack J11 can be noticed in this plot. The suppression of J_c is in order of 10^2 when S is reduced from 4 to 0.16 μm^2 (see Table 5.1). The suppressed J_c of submicron stacks J11 and J24 are shown in the figure 5.3 at 30 K. The curve like structure near zero voltage state is observed. This curve structure is because of insulating behavior of stack at low temperature due to charging effect [16]. The possible mechanism behind this suppression can be the effect of

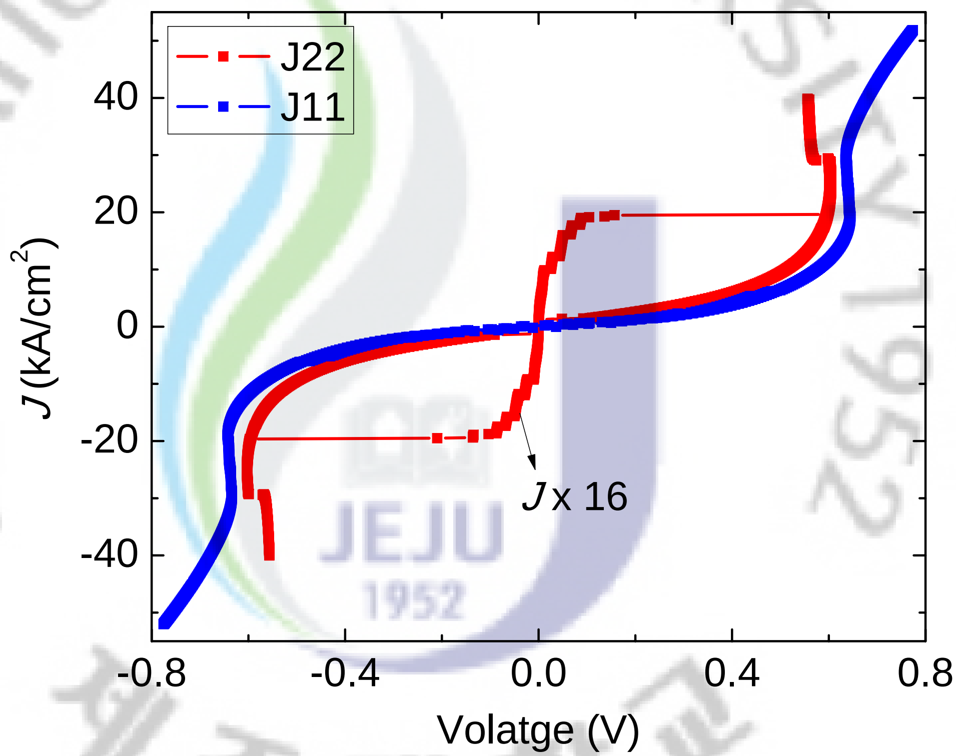

Fig. 5.2: The comparison of J-V characteristics for stack J22 and submicron stack J11 (J22 is plotted on a 16 times expanded scale of J for better comparison)

gallium ion implantation during fabrication process, thermal fluctuations and quantum fluctuations of phase.

Starting with the effect of gallium ions implantation: the gallium ions are penetrated into the surface of stacks up to some distance while fabrication process. The maximum gallium ions penetration depth and area in our experimental conditions of FIB are about 60 nm and 0.01 μm^2 ($4 \times (60)^2$ nm^2), respectively as reported in previous study [17]. The effect of gallium ions cannot be neglected during the fabrication process which can effect J_c. To confirm the effect of gallium ion in J_c, two stacks of same width 0.5 μm, J33 and J11 were fabricated. Both stacks have same level of gallium ion penetration but the value of J_c suppressed only in case of stack J11 (S less than 1 μm^2) (see Table 5.1). This observation concludes that the gallium ion implantation did not contribute in the suppression of J_c in our case. Considering the effect when $k_B T$ is greater than E_J, thermal fluctuations can be a cause for suppression in J_c [18]. The lower limit of critical current value ($\approx 4\pi ekT/h$)

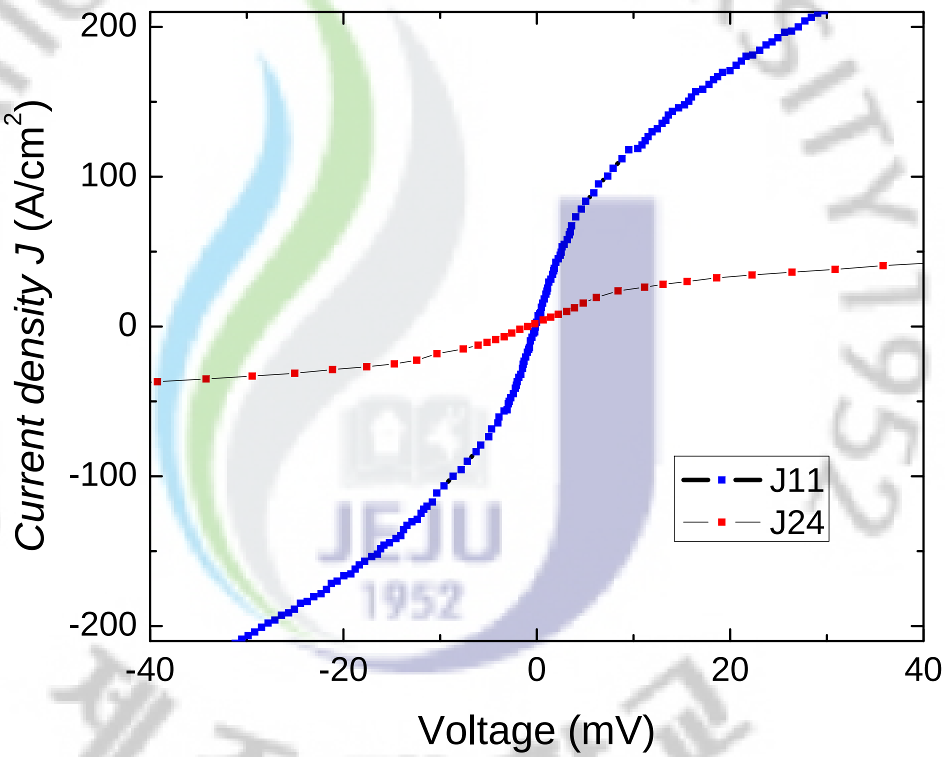

Fig. 5.3: The suppressed J_c in the J-V characteristics along the c-axis of submicron stacks J24 and J11 of Bi-2212 single crystal at 30 K

at 30 K is about 1.2 μA which is an order less than the critical current value for biggest stack (J22 $\approx$ 49 μA). In our case, the value of k_BT is less than the value of E_J as shown in Table 5.1 which eliminate the thermal effect. Interesting feature for submicron stacks is that the hysteresis of the J-V characteristics is suppressed even at low temperature and we have not seen any heating effect at high biasing in J-V characteristics. This analysis shows thermal fluctuations can not be the only mechanism to suppress the J_c.

Now we are extending our analysis for the cause of suppression of J_c on the basis of the quantum fluctuation of phase. The conditions to observe the quantum effects are: E_c should be comparable with the damping rate $\hbar/RC$ and E_J (where R is the resistance and C $(= \epsilon_\circ \epsilon_c S/s)$ is the capacitance) [7]. Mathematically, the first condition $E_c > \hbar/RC$ is fulfilled if the stack area $S < 1\mu\text{m}^2$. Table 5.1 shows the stacks are following the first condition as the value of E_c is greater than $\hbar/RC$.

The second condition to observe quantum effects can be written as an inequality E_J/E_c

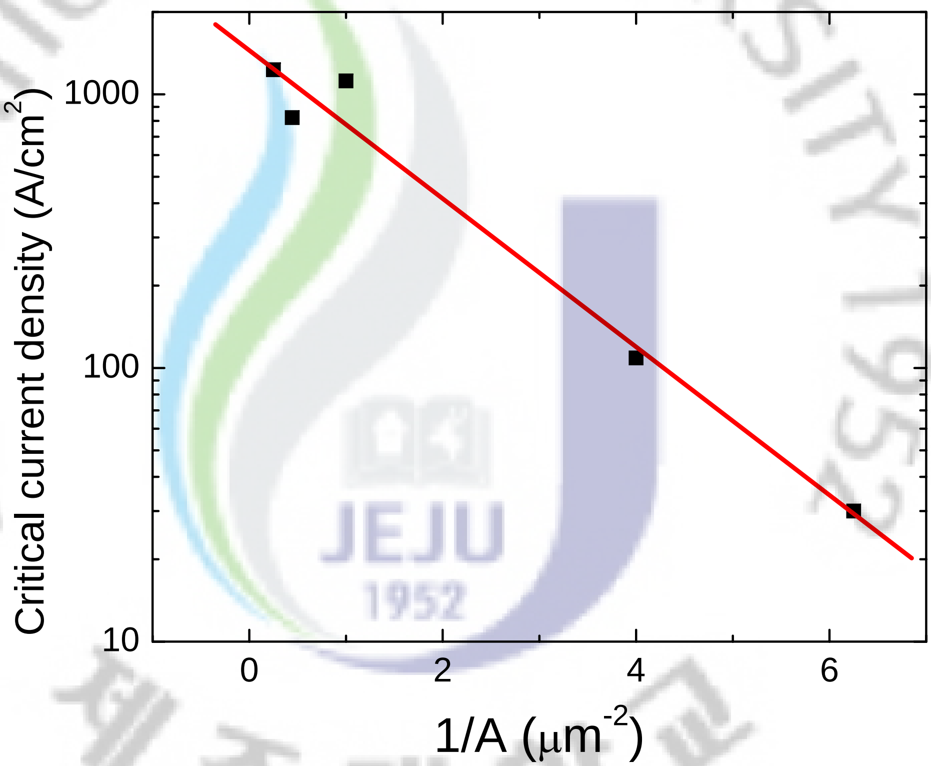

Fig. 5.4: The dependence of critical current density at 30 K upon the inverse area (semi log scale). The squares are our experimental data and the line is an exponential fit of the experimental data.

≤ 1. The value E_J and E_c can be calculated using the relations: $E_J = \Phi_\circ J_{c\circ} S/2\pi$ *and* $E_c = 2e^2 s/\epsilon_\circ \epsilon_c S$, where $\Phi_\circ$ is flux quantum, e is electron charge and $\epsilon_\circ = 5$ is dielectric constant of Bi-2212 along the c-axis [14, 19]. For a single Josephson junction, the condition α ($=E_J/E_c$) ≤ 1 can be rewritten as $S < (4\pi e^2/\Phi_\circ J_c \epsilon_\circ \epsilon_c)^{1/2}$ and as per our experimental conditions, we obtain $S < 0.002\ \mu m^2$. From this value of S, it can be expected that the stacks reported in Table 5.1 might be unaffected by QFs.

However in nano-periodic Josephson junction array of N junctions, E_c can be enhanced by a factor of N because of inter-junction Coulomb interaction [9, 20, 21] and tunneling of Cooper pair. The quantum fluctuations cannot be neglected if $N > 2\alpha^{0.5}$ for the stacks of N IJJs with $\alpha > 1$ [7]. Therefore, the stacks with 100 IJJs quantum fluctuations are effective even if E_J is 10^3 times larger than E_c. Also, to observe quantum effects the value of thermal energy should be smaller than the charging energy. In our case, the value of thermal energy is about 2.6 meV (30 K) which is smaller than the charging energy for submicron stack (J24) 8.8 meV (see Table 5.1).

For further verification, we used equation 5.1 to analyze our data. According to this equation in presence of QFs, the value of J_c drops exponentially as [7, 15, 22]:

$$J(\alpha) \propto exp\left(\frac{N}{2\sqrt{\alpha}}\right) \tag{5.1}$$

since $S \propto \sqrt{\alpha}$, therefore current density should be proportional to *exp(-N/2S)* if there is quantum fluctuation! Taking into account that for our stacks N was nearly constant, we expected J_c to be proportional to exp $(1/S)$, if J_c is affected by quantum fluctuations. So we plotted the $\log(J_c)$ versus $1/S$ as shown in figure 5.4. The observed data show a good agreement with the equation 5.1 as evident from the fitted line. This agreement implies that QFs are responsible for the observed suppression of J_c in junctions having S less than 1 μm^2 as indicated in Table 5.1 and in figure 5.4.

5.4 Conclusions

In conclusion, we have fabricated stack of intrinsic Josephson junctions of Bi-2212 whiskers of different in-plane areas (S) from 4 μm^2 down to 0.16 μm^2. The quantum fluctuations (QFs) in submicron stack at 30 K are observed first time ever. The presence of QFs are verified with strong suppression in critical current density. The conditions to observe quantum effects are discussed. The application of quantum effect can be use in a single electron device at 30 K.

BIBLIOGRAPHY

[1] M. Tachiki, T. Koyama, and S. Uchida *Phys. Rev. B* **50 7065** (1994).

[2] L. Ozyuzer *et al.*, *Science* **318 1291** (2007).

[3] J. Bylander, T. Duty, and P. Delsing, *Nature* **434 361** (2005).

[4] K. K. Likharev, *IBM J. Res. Develop.* **32 144** (1998)

[5] A. Aassime, P. Delsing, and T. Claeson, *Nanotechnology* **12 96** (2001).

[6] L. S. Kuzmin, Yu. V. Nazarov, D. B. Haviland, P. Delsing, and T. Claeson, *Phys. Rev. Lett.* **67 1161** (1991).

[7] L. N. Bulaevskii, A. E. Koshelev, B. Rosenstein, and M.P. Maley, *Physica C* **357 418** (2001).

[8] A. Franz, Y. Koval, D. Vasyukov, P. Muller, H. Schneidewind, D. A. Ryndyk, J. Keller, and C. Helm, *Phys. Rev. B* **69 014506** (2004).

[9] D. B. Haviland, K. Anderson, and P. Agren, *J. Low temp. Physics* **118 733** (2000).

[10] M. Nagao, M. Sato, H. Maeda, S. -J. Kim, and T. Yamashita, *Appl. Phys. Lett.* **79 2612**(2001).

[11] S.-J. Kim, Yu. I. Latyshev, and T. Yamashita, *Supercond. Sci. Technol.* **12 729** (1999).

[12] S. Saini, G. S. Kim, S.-J. Kim, *J. Supercond. Nov Magn* **23 811** (2010).

[13] A. A. Levin, I. Y. Smolin, F. Y. Shepelev, *J. Phys. Condens.Matter* **6, 3539** (1994).

[14] Yu. I. Latyshev, S. -J. Kim, and T. Yamashita *JETP Lett.* **69 84** (1999).

[15] P. A. Warburton, J. C. Fenton, M. Korsah, and C. R. M. Grovenor, *Supercond. Sci. Technol.* **19 S187** (2006).

[16] P. Delsing, C. D. Chen, D. B. Haviland, Y. Harada, and T. Claeson, *Phys. Rev. B* **50 3959** (1994).

[17] S. -J. Kim, Yu. I. Latyshev, and T. Yamashita, *Appl. Phys. Lett.* **74 1156** (1999).

[18] M. Tinkham, *Introduction to Superconductivity 2nd edn (New York:McGraw-Hill) Chap.7* (1996).

[19] The value of E_J is calculated using unfluctuated critical current density ($J_{c\circ}$) and presented in Table 5.1. The value of J_c, showed in Table 5.1, is the measured value of critical current density and used in figure 5.4.

[20] K. K. Likharev *et al*, *IEEE Trans. Magn.* **25 1436** (1989).

[21] K. K. Likharev and K. A. Matsuoka, *Appl. Phys. Lett.* **67 3037** (1995).

[22] The equation represents a relation between critical current density and alpha in presence of quantum fluctuations. The quantum regime can be achieved by two ways i) to decrease the Josephson energy, ii) to increase charging energy. In most of the cases people try to suppress the critical current and decrease the value of Josephson energy using magnetic field. In our case, we increase the value of charging energy by decreasing the in-plane area of stacks, which lead to quantum fluctuation effects. In Bulaevskii et al [7], they described the crossover to see the quantum regime using magnetic field. The use of magnetic field is to observe the effect of quantum fluctuation which means the relation of critical current density and alpha will be valid if quantum fluctuations exist and do not depend how the quantum fluctuations are generated. Hence the equation can be applicable in both magnetic and non-magnetic field cases.

6. CHARACTERISTICS OF SUBMICRON JOSEPHSON JUNCTIONS OF Y123/PR123 MULTI LAYERED THIN FILMS

We fabricated intrinsic Josephson junctions (IJJs) in *a*-axis oriented Y123 thin film of thickness about 500 nm. IJJs (CuO_2 planes) were aligned perpendicular to the substrate in the thin films. The bridge type pattern was fabricated using focused ion beam milling technique in such a way that the current flow along the *c*-axis in thin film. The dimensions of bridge were about 1 μm $\times$ 5 μm. The value of T_c and J_c for micron bridge are about 89 K and 2×10^6 A/cm^2 at 10 K, respectively. The samples were irradiated with external microwave at 20 GHz and the J_c was suppressed with increase in power. This suppression in J_c indicates the formation of layered structure with strong coupling. The voltage steps were appeared with microwave irradiation in I-V characteristics. The value of voltage steps were irregular and change with increase in power. The *dc*-Josephson current relation shows formation of superconducting-insulating-superconducting type Josephson junctions in micron bridge.

To extend our study, we have also fabricated a submicron stack in *a*-axis oriented multi layered thin films of $YBa_2Cu_3O_7$ (Y123) and $PrBa_2Cu_3O_7$ (Pr123) using three dimensional focused ion beam milling technique in such a way that the current was forced to flow along Josephson junctions in multi layered thin film. The in-plane of the stack is about 300 nm $\times$ 200 nm. The transition temperature (T_c) and critical current density (J_c) of submicron stack were about 70 K and 2×10^5 A/cm^2 at 30 K, respectively. The stack was irradiated with external microwave of 10 GHz with different power and studied at 30 K. The supercurrent branch become resistive above a certain microwave power and also the J_c was suppressed as we increased the microwave power. The temperature dependence of dc-Josephson current relation was analyzed with Ambegaokar-Baratoff (A-B) theory. The relation shows formation of superconducting-semiconducting-superconducting type Josephson junctions.

6.1 Introduction

High T_c superconductors (HTSCs) $REBa_2Cu_3O_y$ (RE-123), where RE denotes rare earth element, are the most fascinating material for second-generation superconducting devices. $YBa_2Cu_3O_7$ (Y123) is one of the HTSC family superconductor having lattice parameters of a = 3.82 Å, b = 3.88 Å, c = 11.68 Å [1]. The orientation of Y123 thin film can be controlled in any axis from a-axis to c-axis. Y123 can be a prospective candidate for nano device fabrication because of high T_c and higher value of critical current [2, 3]. A-axis oriented thin films are potentially superior to c-axis films for sandwich-type junction applications because of the larger coherence length in a-axis direction [4]. Thus growth of thin epitaxial insulators or normal barriers on a-axis films, followed by another a-axis superconductor, is an important goal. The layered structure of superconducting Y123 gives the phenomenon of intrinsic Josephson junctions (IJJs) and these junctions are arranged as an array along the c-axis.

The application of microwave irradiation on IJJs can be use in the quantum electronics [5]. The IJJs are very sensitive to the external electromagnetic environments and when it is irradiated by microwave a constant voltage plateaus appear in current-voltage (I-V) characteristics in a sequence of equality separated voltage [6, 7, 8]. The dynamics of vortex can be one of the causes for these steps. In case of array of Josephson junctions the steps appear in giant value and show the collective response of many Josephson junctions. The suppression in critical current takes place when microwave is irradiated. This unique property of Josephson junction can be apply in many applications such as superconducting quantum interface device (SQUID), high frequency devices, voltage standard, photon detection, and many more. In this study, we have used a-axis oriented Y123 thin films which works as the Josephson junctions array along the parallel direction to the substrate (c-axis). The devices were fabricated using 3-D focused ion beam (3D FIB) milling

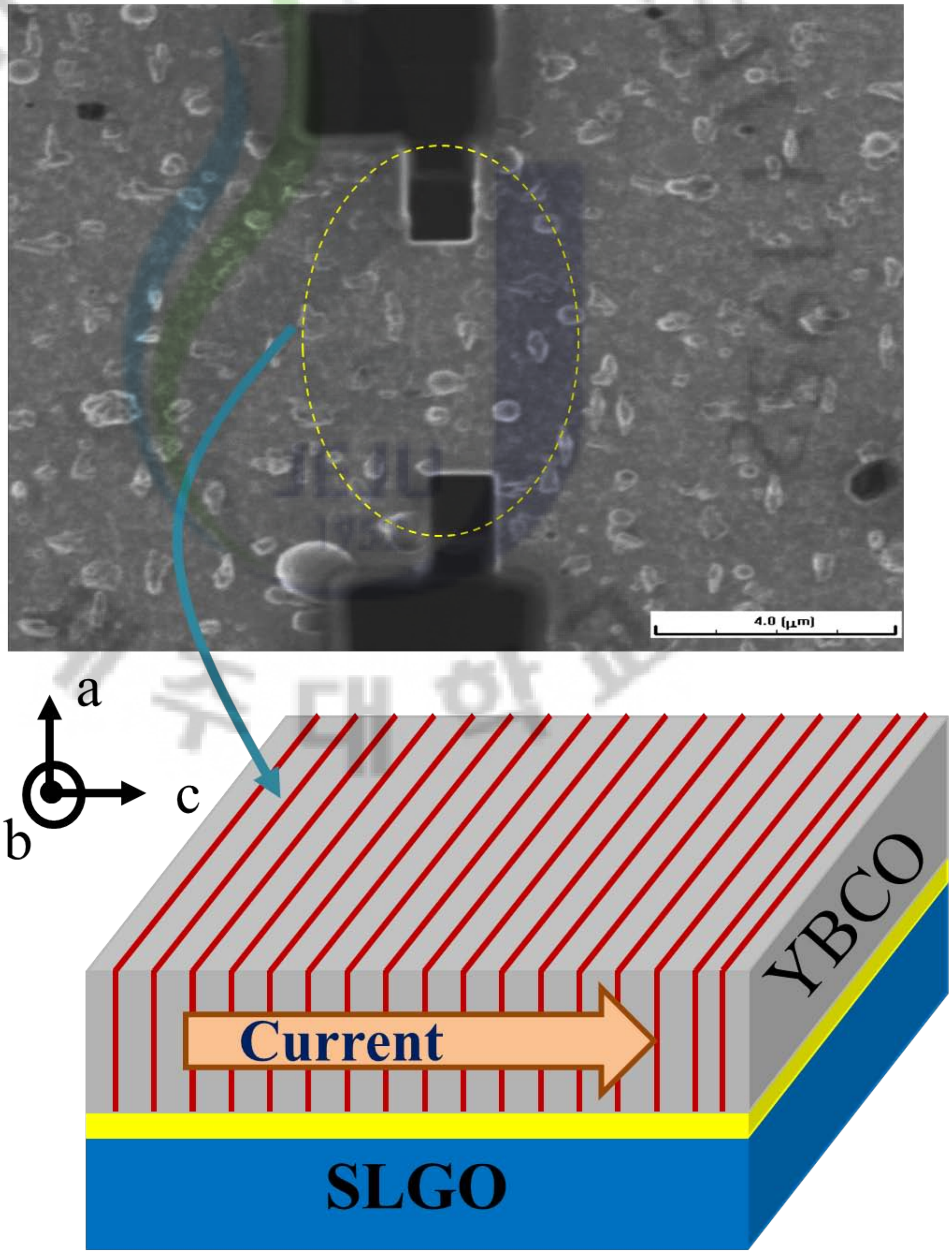

Fig. 6.1: FIB image of micro-bridge (scale bar of 4 μm) and schematic of the IJJs configuration in the micro-bridge fabricated on a-axis oriented Y123 thin films. The arrow indicates the direction of current to observe IJJs. The axial direction of thin film is shown in the inset.

technique. The I-V characteristics have been measured for devices with microwave irradiation. Devices show the response with microwave irradiation in different power and critical current suppress as increase microwave power.

6.2 Experimental details

6.2.1 Growth of a-axis oriented multi layered thin films

The a-axis oriented Y123/Pr123 multi layered thin films were grown on (100) $SrLaGaO_4$ (SLGO) substrates with buffer layer of Gd_2CuO_4(Gd214) by a pulse laser deposition (PLD) technique using ArF excimer laser (by Dr M. Takamura and Prof M Mukaida, Department of Material Science and Engineering, Kyushu University, Japan). The thickness of Y123 and Pr123 is about 50 nm and 10 nm respectively in multi layered thin films. The detail recipe of growth of thin films have described elsewhere [9]. A sintered target with 38 mm in diameter and 4 mm in thickness of Y123/Pr123 and Gd214 is used to grow the thin films. The targets are rotated during the irradiation of laser beam. The SLGO substrate were glued with silver epoxy on a substrate heater specially designed for ultrahigh vacuum applications. First of all, the buffer layer of Gd214 of 50 nm were deposited on clean surface of SLGO substrate at 730 °C in a 40 mTorr oxygen pressure. After the buffer layer, alternate Y123 and Pr123 thin films of thickness 15 nm and 5 nm respectively were deposited at 700 °C. The deposition parameter such as deposition temperature of films is in the range of 680 - 700 °C, pulse frequency is 5 Hz, and rotation speed of the target is about 0.5 rpm. We grow two types of film; i) a-axis oriented Y123 thin films for IJJs study (micron bridge) and ii) a-axis oriented Y123/Pr123 multi layered thin films for submicron Josephson junctions (submicron stack).

6.2.2 Fabrication of submicron stack of a-axis oriented multi layered thin films

We have fabricated submicron stack using 3-D FIB machine (SII NanoTechnology SMI2050), operating with a Ga^+ ion beam of energy 30 KeV and beam current from 1 pA to 20 nA in thin films. The detail fabrication technique is described in our previous reports [10, 11].

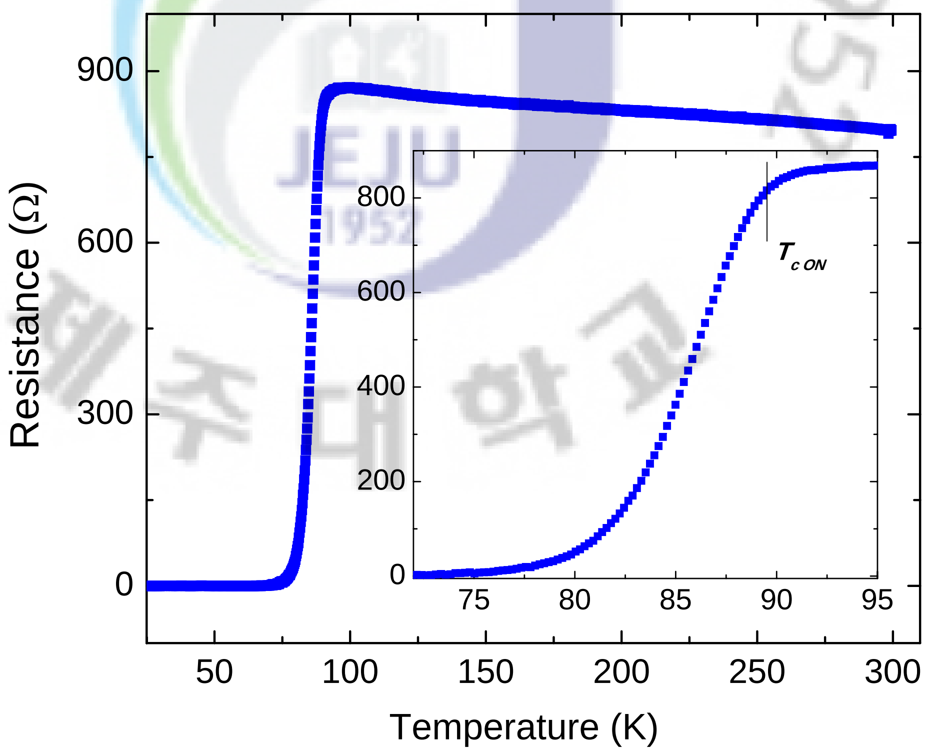

Fig. 6.2: The R-T characteristics of micro-bridge fabricated in a-axis oriented Y123 thin films. Transition temperature starts about 89 K. Inset shows enlarge area near the transition temperature.

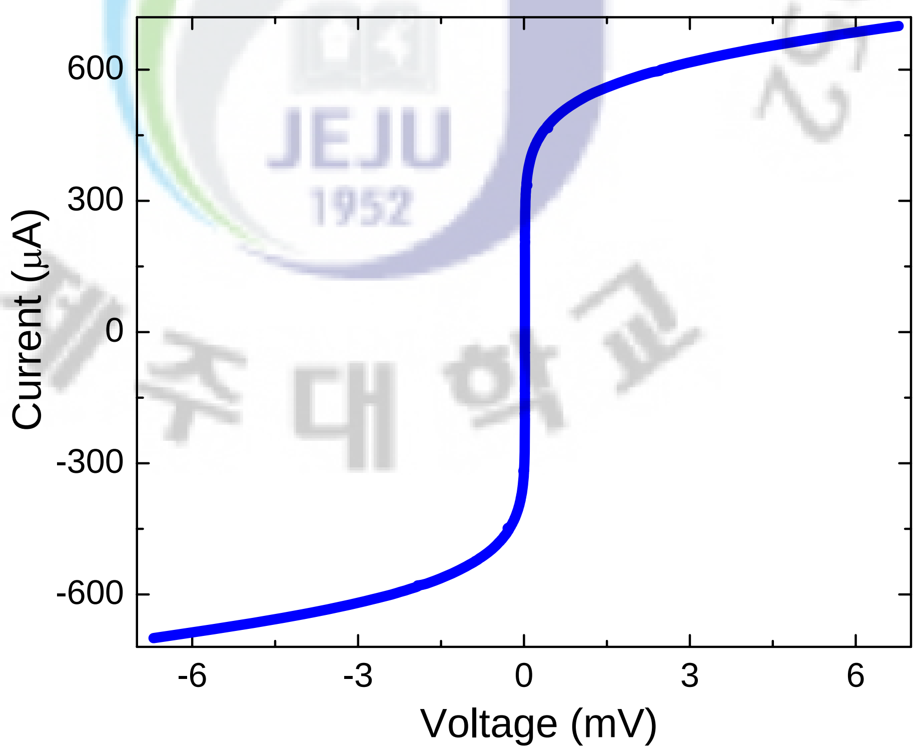

Fig. 6.3: The I-V characteristics of micro-bridge fabricated in a-axis oriented Y123 thin films at 10 K without microwave irradiation.

Briefly in this process, the FIB machine has a freedom of tilting and rotating the sample stage up to 60° and 360° respectively. We used a sample stage that itself inclined by 60° with respect to the direction of the ion beam. We tilted the sample stage by 30° so that the sample was set to be perpendicular to the ion beam and the sample was milled along the *bc*-plane. We turned sample stage back to the initial orientation and rotated it by 180° so that the incline plane was set to be 60° with respect to the ion beam. We then tilted sample stage by 60° so that the sample was set to be perpendicular to the ion beam and the sample was milled along the *ac*-plane of the multi layered thin film. The in-plane area of submicron stack is about 200 nm × 300 nm. The number of Josephson junctions is 12 in the multi layered thin film and at least two Josephson junctions belong in submicron stack as the height of stack is about 240 nm. The micron bridge is fabricated in *a*-axis oriented Y123 thin films by etching only in in-plane, the dimensions are about 1 μm along the *c*-axis and 4 μm along the *b*-axis of thin film. Intrinsic Josephson junctions are aligned along the *c*-axis of *a*-axis oriented Y123 thin films. The detailed fabrication process is discribed in chapter 3. For electric transport characterization, Keithley AC-DC source 6221 and Keithley nano voltmeter 2182A are used. The resistance-temperature (R-T) characteristics and current-voltage (I-V) characteristics are performed using four probe technique. Low pass filters are used in signal line to reduce the external noise.

6.3 Results and discussion

Figure 6.1 shows FIB image of micro-bridge fabricated on *a*-axis oriented Y123 thin film. The expended view shows schematic diagram of array of IJJs in micro-bridge with a buffer layer of Gd214 (50 nm) on SLGO substrate. The direction of flow of current in micro-bridge is along the *c*-axis and shows a combined effect of array of IJJs. The dark lines perpendicular to substrate indicate the CuO planes. The layered structure with CuO planes forms IJJs. The micro-bridge is in such a way that current flows across these junctions and the Cooper pairs tunnel through these barriers. The R-T characteristic of micro-bridge of *a*-axis oriented Y123 is shown in figure 6.2 and transition temperature (T_{cON}) is about 89 K (where T_{cON} is the temperature from where superconductivity state starts). Before T_{cON}, micro-bridge shows the usual semiconducting behavior along the

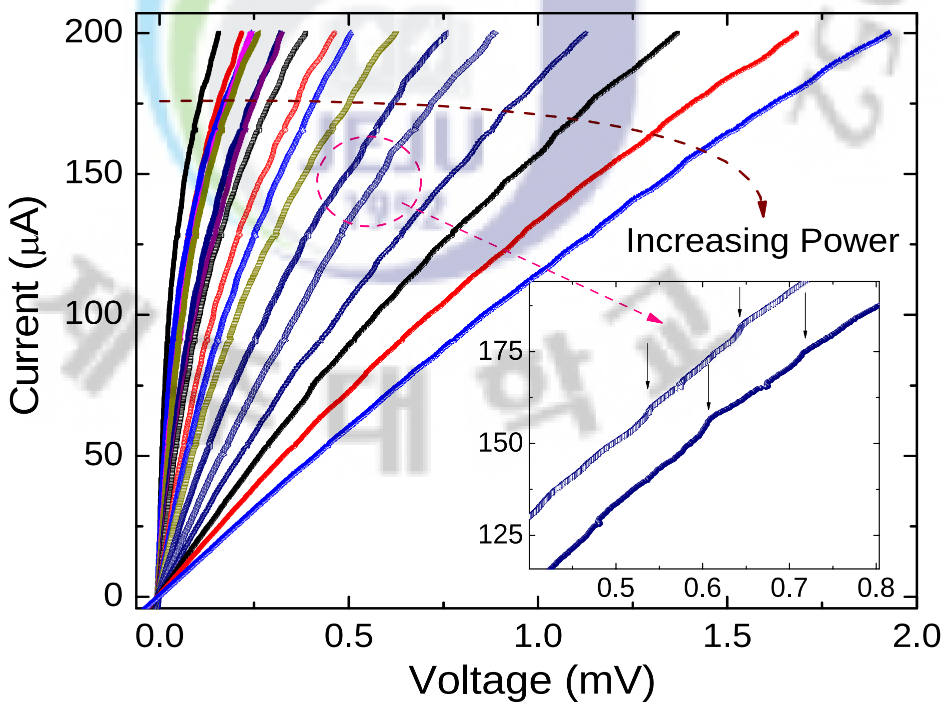

Fig. 6.4: The I-V characteristics of micro-bridge at 20 GHz frequency of microwave irradiation of different power at 65 K. Inset shows the voltage steps at the indicated region.

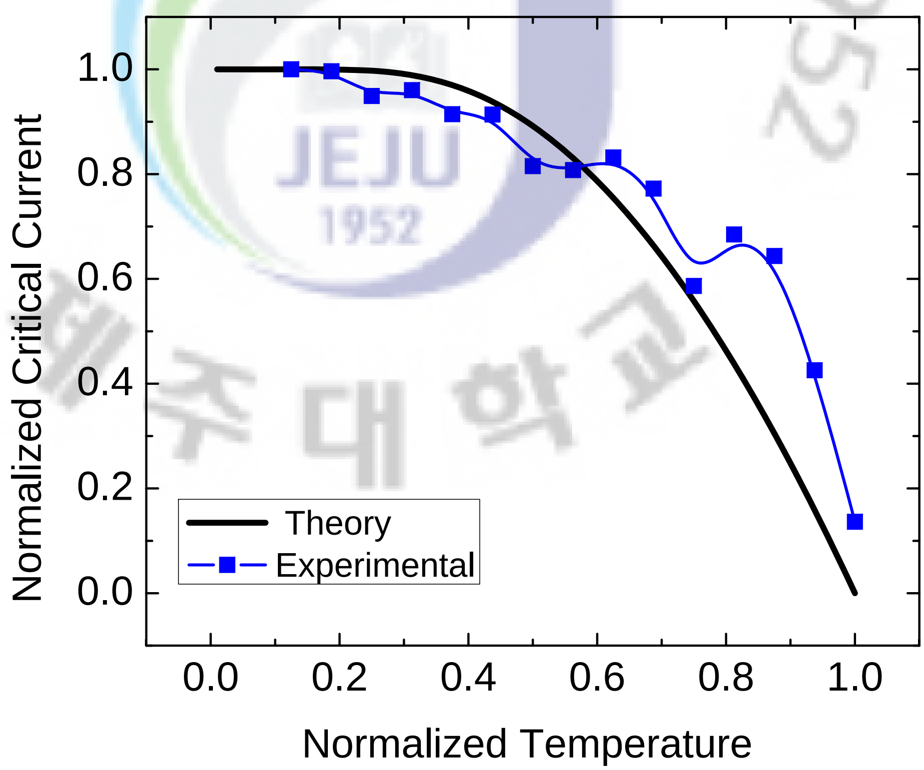

Fig. 6.5: Comparison of experimental data (solid square points) with the theoretical estimation of A-B theory for micro-bridge fabricated in a-axis oriented Y123 thin films.

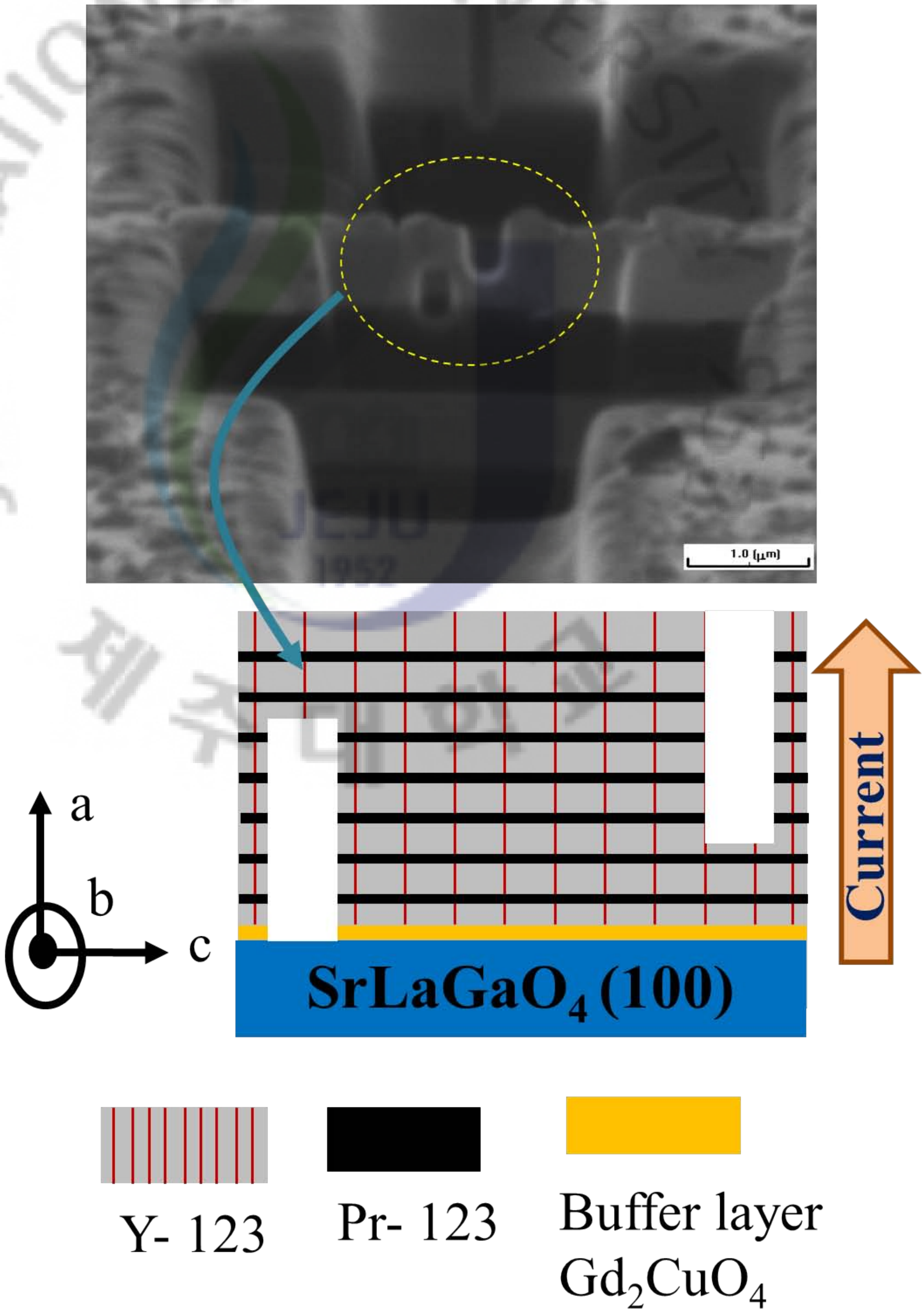

Fig. 6.6: FIB image of submicron stack (scale bar of 4 μm) and schematic of the JJs configuration in the submicron stack fabricated on a-axis oriented Y123/Pr123 multi layered thin films. The arrow indicates the direction of current to observe IJJs. The axial direction of thin film is shown in the expended view.

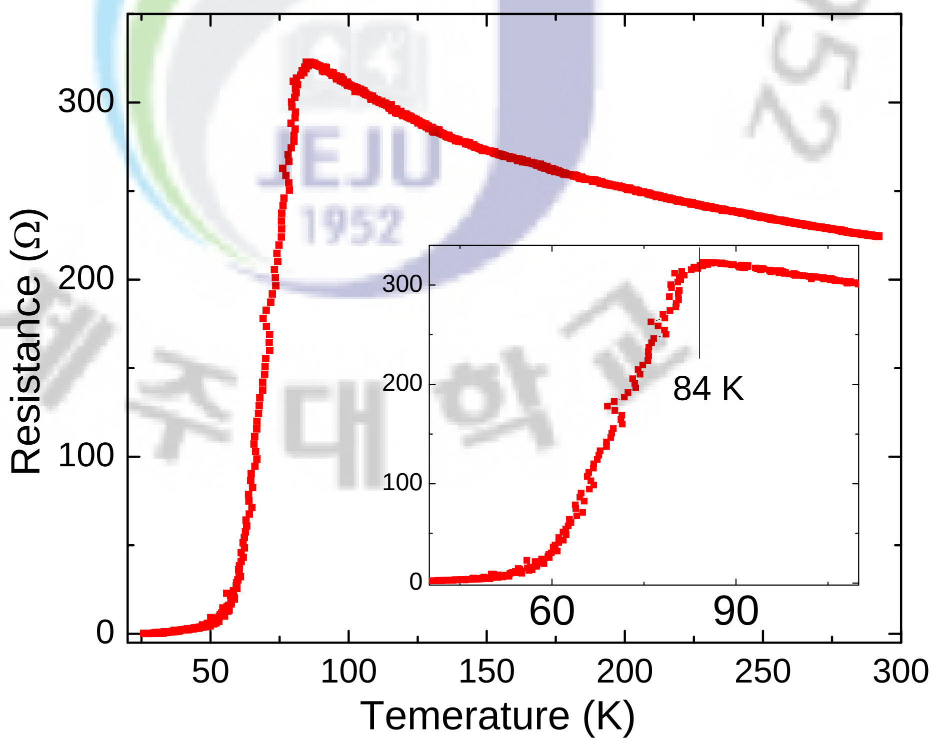

Fig. 6.7: The R-T characteristics of submicron stack fabricated in a-axis oriented Y123/Pr123 multi layered thin films. Transition temperature starts about 84 K. Inset shows enlarge area near the transition temperature.

c-axis.

The super current branch in I-V characteristics corresponds to all IJJs in micro-bridge and the number of IJJs can be calculated (N = length of micro-bridge/1.16 nm) about 833. The critical current density (J_c) of about 2×10^6 A/cm^2 has been calculated from I-V characteristics at 10 K without external microwave irradiation. We have not found any hysteresis in I-V characteristics. The I-V characteristics of micro-bridge fabricated in a-axis oriented Y123 thin films at 10 K without microwave irradiation shown in figure 6.3.

We measure I-V characteristics with external microwave irradiation of 20 GHz and different power at 65 K. Figure 6.4 shows the effect of microwave irradiation on micro-bridge. With increasing microwave power, the critical current (I_c) has suppressed gradually. The power of microwave has increased vortices in IJJs and caused suppression of I_c. The suppression in I_c shows the effect of microwave. The maximum suppression is occurring at maximum power of 20 GHz frequency of microwave. The superconducting branch is sensitive to the microwave power. The value of I_c suppress with increase in the microwave power. The microwave power is varied from 0 dbm to 15 dbm in the step of 2.5 dbm. The super current branch become resistive above a certain microwave power.

The microwave induced voltage steps have been appeared in I-V characteristics with different power. The voltage steps are clearer as we increase the biasing voltage. The value of voltage steps are increasing with increase in power. The relation with power indicates these voltage steps are induced because of flux flow behavior of Josephson vortex.

The temperature dependence of critical current density ($J_c - T$) has been fitted with the Ambegaokar-Baratoff (A-B) theory. The fitted curve with experimetal data indicates towards superconductor-insulator-superconductor (SIS) type Josephson junction [12]. Figure 6.5 shows the temperature dependence of normalized critical current ($\mathrm{I}_c/\mathrm{I}_{cat10K}$). The solid blue squares are the experimental data and the line is theoretical estimation of A-B theory. The experimental data are well fitted with theoretical estimation.

We have extended our study of a-axis oriented Y123 films to a-axis oriented multi layered Y123/Pr123 thin films. Figure 6.6 shows FIB image of submicron stack fabricated in a multi layered Y123/Pr123. The number of Pr123 layers is 36 in multi layered thin films. The thickness of Pr123 and Y123 are about 5 nm and 15 nm, respectively. The schematic diagram of multi-layered thin films is also shown in the figure. The axial orientation of multi-layered thin films is shown in inset. We have used the current direction as shown by the arrow to observe the Josephson junction effect. The films are deposited on $SrLaGaO_4$ substrate with buffer layer of 50 nm Gd_2CuO_4. The dimensions of submicron stack in-plan area are 0.3 μm $\times$ 0.2 μm with height of 200 nm. In the stack Pr123 layer works as a semiconducting layer and Y123 works as a superconducting electrode. This layered structure is a superconducting-semiconducting-superconducting type Josephson junction.

Figure 6.7 shows the R-T characteristics of multi layered thin film of Y123/P123. We find transition temperature ON (T_c) of about 84 K. Inset of figure 6.7 shows the magnified region near the transition temperature. The value of T_c for submicron stack has found lower than the pure a-axis oriented Y123 thin film which is the effect of Pr123 layered sandwiched with Y123.

The I-V characteristics of submicron stack fabricated on multi layered thin film of Y123/P123 is shown in figure 6.8 at 30 K. The supercurrent branch shows a tilte because of resistance which can be confirm from the R-T characteristics. Further we have measured the I-V characteristics of submicron stack with different power of 10 GHz microwave frequency at 30 K. Figure 6.9 shows the I-V characteristics of submicron stack with 10 GHz of microwave frequency at different power at 30 K. The critical current has suppressed as we apply any microwave power. The suppression of critical current indicates that the microwave is suppressing superconductivity and pinning in the submicron stack. We calculate critical current about 0.12 mA from I-V characteristics at 30 K without any microwave irradiation. The suppression in critical current has occurred when we apply the microwave with any power. The maximum suppression is occurring at +15 db power of 10 GHz frequency of microwave. The voltage steps have not appeared in the I-V characteristics which can be the cause of fabrication technique and quality of multi layered film. However, the suppression in critical current shows the effect of microwave irradiation in Josephson junctions.

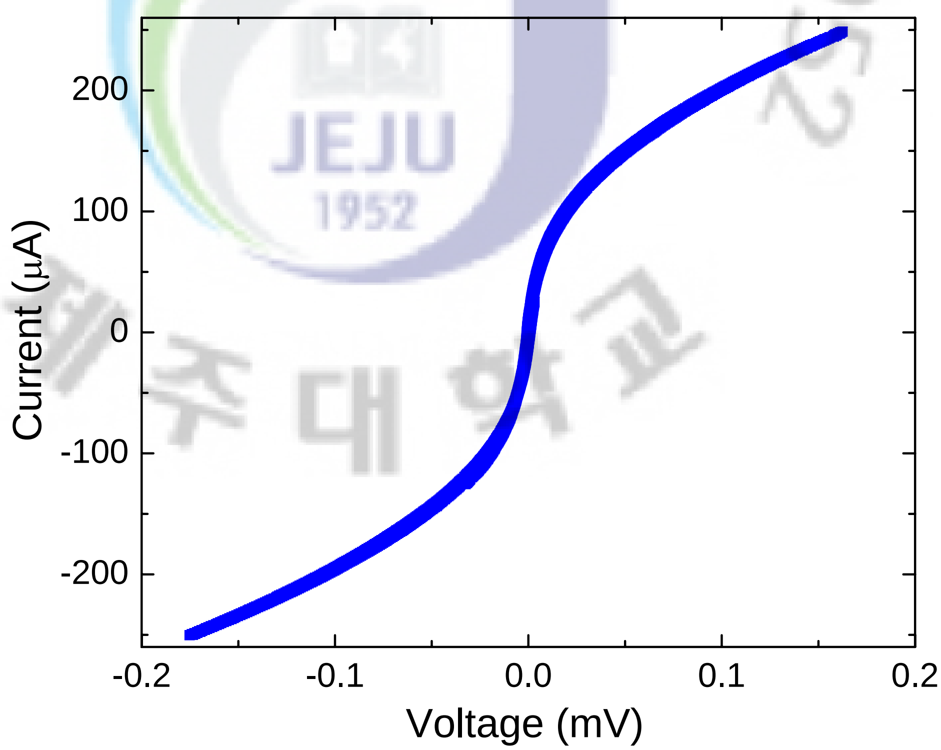

Fig. 6.8: The *I*-*V* characteristics of submicron stack fabricated in *a*-axis oriented Y123/Pr123 multi layered thin films at 30 K without microwave irradiation.

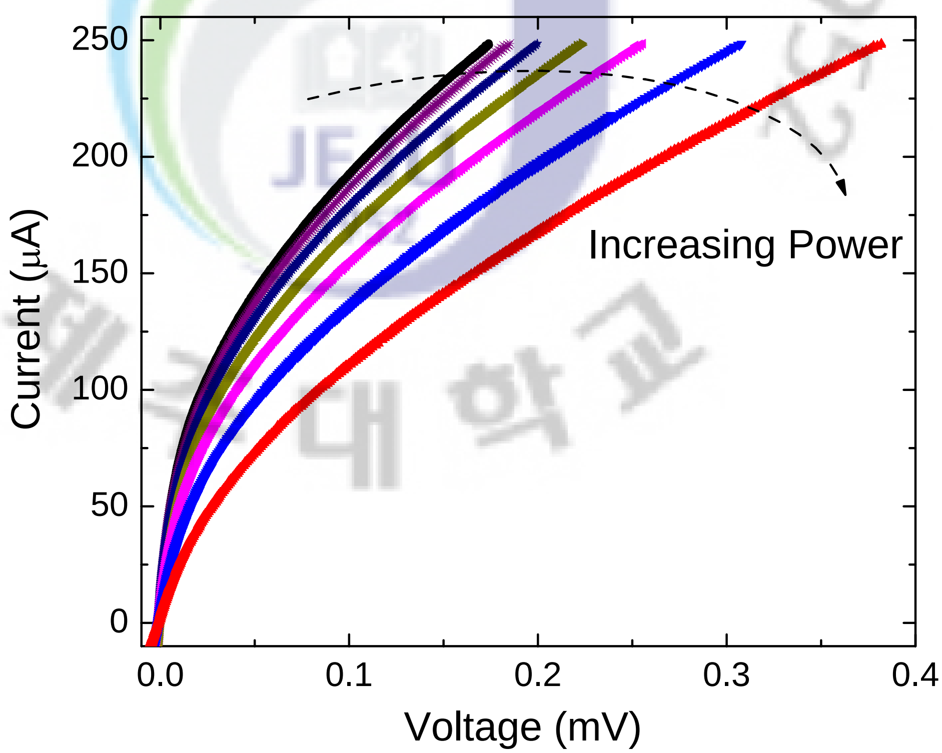

Fig. 6.9: The I-V characteristics of submicron stack at 10 GHz frequency of microwave irradiation of different power from 0 to +15 dbm in the steps of 2.5 dbm at 30 K.

6.4 Conclusion

We have fabricated a micro-bridge (in a-axis oriented $YBa_2Cu_3O_7$ thin films) and submicron stack (in a-axis oriented $YBa_2Cu_3O_7/PrBa_2Cu_3O_7$ multi layered thin films) using 3-D FIB etching technique to observe Josephson junctions characteristics. The transition temperature for micro-bridge is about 89 K. The critical current of about 2×10^6 A/cm^2 has calculated at 10 K from I-V characteristics. We notice suppression in critical current as the effect of external microwave at different power. As we increase the power, the superconducting state is suppressing and results to suppress the critical current. The value of flux flow voltage steps are increasing with increase in power of microwave. To extend our study, a submicron stack has been fabricated in multi layered thin films of Y123/Pr123 and submicron stack gives response with microwave irradiation. We believe these results give scope for future analysis to grow the multi-layered thin film of all a-axis oriented $YBa_2Cu_3O_7$ and $PrBa_2Cu_3O_7$ for high frequency device applications.

BIBLIOGRAPHY

[1] S. W. Tozer, A. W. Kleinsasser, T. Penney, D. Kaiser, and F. Holtzberg, *Phys. Rev. Lett.*, **59, 1768** (1987).

[2] Y. Shingai, M. Mukaida, K. Matsumo, Y. Yoshida, A. Ichinose, S. Horii, A. Saito, and S. Ohsima, *Physica C*, **412, 1296** (2004).

[3] Z. Trajanovic, I. Takeuchi, C.J. Lobb, T. Venkatesan, and P.A. Warbutron, *IEEE Transactions on Applied Superconductivity*, **7, no. 2, 1636** (1997).

[4] T. K. Worthington, W. J. Gallagher, and T. R. Dinger, *Phys. Rev. Lett.*, **59, 1160** (1987).

[5] C. P. Foley and H. Hilgenkamp, *Supercond. Sci. Technol.*, **22, 064001(1-5)** (2009).

[6] S. Shapiro, *Phys. Rev. Lett.*, **11, 80** (1963).

[7] S. Shapiro, A. Janus, and S. Holly, *Rev. Mod. Phys.*, **36, 223** (1964).

[8] A. Irie, Y. Hirai, and G. Oya, *Appl. Phys. Lett.*, **72, 2159** (1998).

[9] M. Takamura, M. Mukaida, S. Horii, A. Inchinose, R. Kita, K. Matsumoto, Y. Yoshida, M. Namba, S. Awaji, K. Watanabe, R. Teranishi, and N. Mori, *Supercond. Sci. Technol.*, **23, 045023(1-4)** (2010).

[10] S. -J. Kim, Yu. I. Latyshev, and T. Yamashita, *Supercond. Sci. Technol.* **12 729** (1999).

[11] S. Saini, G. S. Kim, and S.-J. Kim, *Jpn. J. Appl. Phys. 49, 04DJ13 (1-3)* (2010).

[12] V. Ambegaokar and A. Baratoff, *Phys. Rev. Lett.* **10, 486** (1963).

7. MICROWAVE IRRADIATION ON A-AXIS ORIENTED Y123/PR123 NANO-SQUID

A submicron superconducting quantum interference device was fabricated in vertical Josephson junctions of a-axis oriented $YBa_2Cu_3O_7$ and $PrBa_2Cu_3O_7$ (Y123/Pr123) multi layered thin films using three dimensional focused ion beam milling technique. The transition temperature and critical current density (J_c) of the device are about 83 K and 2 $\times$ 10^6 A/cm^2 at 20 K, respectively. The device was irradiated with external microwave up to 40 GHz and studied at 20 K. The microwave induced voltage steps are observed in I-V characteristics. The super current branch become resistive above a certain microwave power and also the J_c was suppressed as we increased the microwave power. The temperature dependence of dc-Josephson current relation was verified with Ambegaokar-Baratoff (A-B) theory. The relation shows formation of superconducting-semiconducting-superconducting type Josephson junctions.

7.1 Introduction

Since the discovery of the layered high-T_c superconductors (HTSCs) $REBa_2Cu_3O_y$ (RE123, RE denotes rare earth elements), it has been accepted one of the most fascinating material for second-generation superconducting devices using Josephson junction phenomenon. Highly anisotropic $YBa_2Cu_3O_7$ (Y123) is one of the HTSC family superconductor having higher electrical conductivity in ab- plane than c-axis [1]. The orientation of Y123 thin film can be controlled in any axis from a-axis to c-axis [2]. A-axis oriented thin films are potentially superior to c-axis films for sandwich-type junction applications because of the larger coherence length in a-axis direction [3]. Thus growth of thin epitaxial insulators or normal barriers on a-axis films, followed by another a-axis superconductor, is an important goal. The application of microwave irradiation on such multi layered thin film Josephson junctions (JJs) can be used in the quantum electronics [4]. These JJs are very sensitive to the external electromagnetic environments. A constant voltage plateaus appear in current-voltage (I-V) characteristics in a sequence of equally separated voltage when JJs are irradiated by external microwave [5, 6, 7]. The dynamics of vortices under the influence of external microwave can be one of the reason for the occurance of these steps. This unique property of JJs can be apply in many applications such as superconducting quantum interface device (SQUID), high frequency devices, voltage standard, photon detection, and many more [8, 9, 10, 11, 12, 13].

In this study, we have used a-axis oriented Y123 and $PrBa_2Cu_3O_7$ (Pr123) multi layered thin films which work as the Josephson junctions across the multi layered thin films (a-axis of thin films). The submicron SQUID devices are fabricated using 3-D focused ion beam (3D FIB) milling technique. The I-V characteristics have been measured for devices with microwave irradiation. The device shows the response of microwave irradiation in different power and the value of critical current suppress with increase in microwave power.

7.2 Experimental details

7.2.1 Growth of multi layered thin films of a-axis oriented Y123/Pr123

The a-axis oriented Y123/Pr123 multi layered thin films were grown on (100) $SrLaGaO_4$ (SLGO) substrates with buffer layer of Gd_2CuO_4(Gd214) by pulse laser deposition (PLD) technique using ArF excimer laser (by Dr. M. Takamura and Prof. M. Mukaida, Department of Material Science and Engineering, Kyushu University, Japan). The detail recipe of growth of thin films have been described elsewhere [14]. Briefly, a sintered target with 38 mm in diameter and 4 mm in thickness of Y123 and Gd214 is used to grow the thin films. The targets are rotated during the irradiation of laser beam. The SLGO substrate were glued with silver epoxy on a substrate heater specially designed for ultrahigh vacuum applications. First of all, the buffer layer of Gd214 of 50 nm were deposited on clean

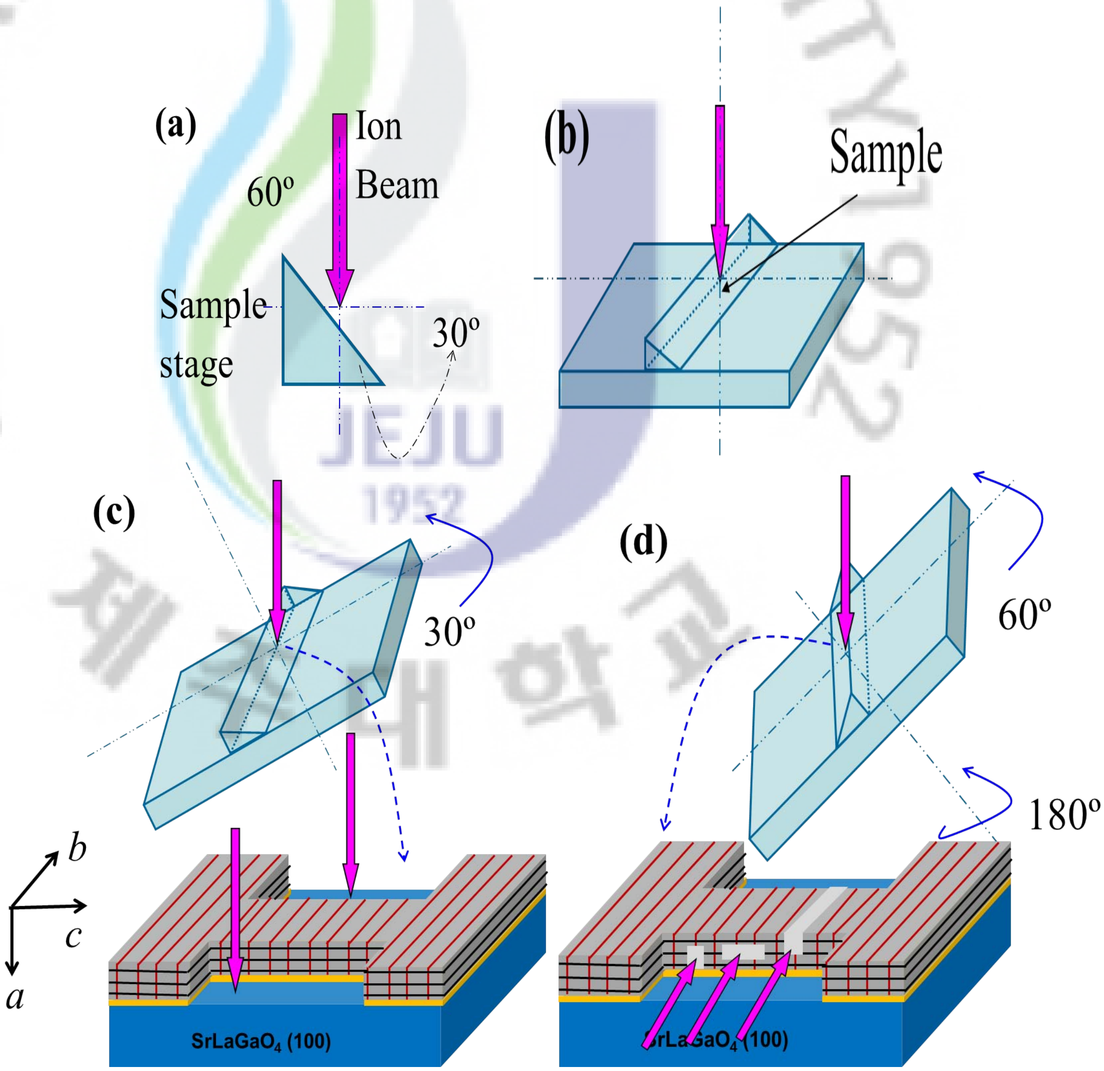

Fig. 7.1: Scheme of 3-D FIB milling process (a) The incline sample stage plane has an angle of 60° with ion beam (where we mount sample). (b) The initial orientation of sample and sample stage. (c) Sample stage titled by 30° anticlockwise with respect to ion beam and milling along *bc*-plane of the mulilayered thin film. The axis notation indicates the orientation of multi layered thin films. (d) The sample stage rotated by an angle of 180° and also tilted by 60° anticlockwise with respect to ion beam and milled along the *ac*-plane of the mulilayered thin film.

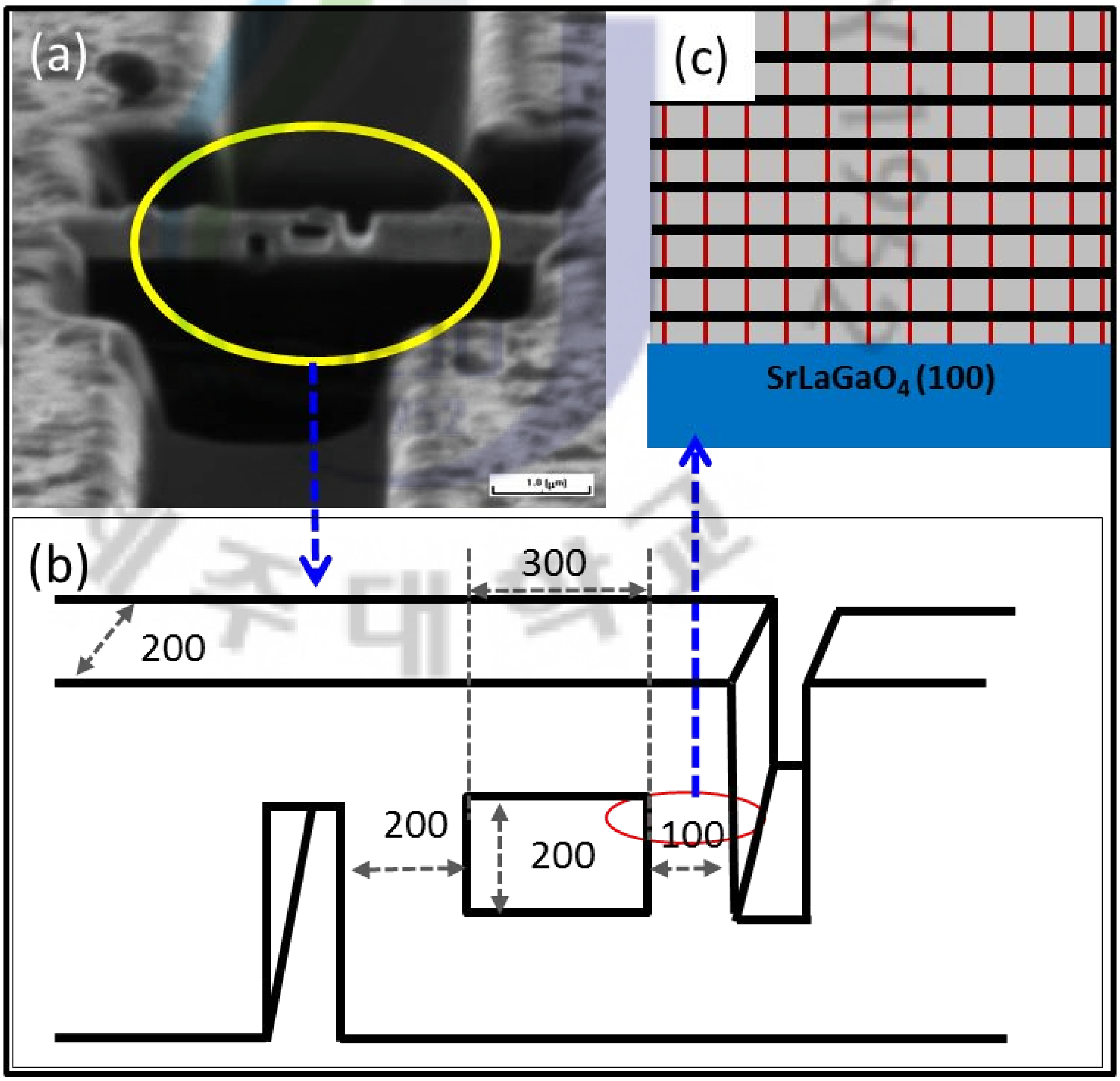

Fig. 7.2: (a) FIB image of submicron-SQUID device in Y123/Pr123 multi layered thin films; (b) The schematic of fabricated device (all dimensions are in nm); (c) The schematic shows alignment of CuO planes in multi layered Y123/Pr123.

surface of SLGO substrate. After the buffer layer, we deposited alternate Y123 and Pr123 thin films of thickness 15 nm and 5 nm respectively. The deposition parameter such as deposition temperature of films is in the range of 680 - 700 °C, pulse frequency is 5 Hz, and rotation speed of the target is about 0.5 rpm.

7.2.2 Fabrication of SQUID structure in a-axis oriented Y123/Pr123

We have fabricated devices using 3-D FIB machine (SII NanoTechnology SMI2050), operating with a Ga^+ ion beam of energy 30 KeV and beam current from 1 pA to 20 nA in thin films. The detail fabrication technique is described in our previous report [15, 16]. Brifly in this process, the FIB machine has a freedom of tilting and rotating the sample stage up to 60° and 360° respectively. We used a sample stage that itself inclined by 60° with respect to the direction of the ion beam (as shown in figure 7.1 (a)). We tilted the sample stage by 30° so that the sample was set to be perpendicular to the ion beam and the sample was milled along the bc-plane (as shown in figure 7.1 (c)). The axis notation in inset of figure 7.1 (c) shows the orientation of multi layered thin film. We turned sample stage back to the initial orientation and rotated it by 180° so that the incline plane was set to be 60° with respect to the ion beam. We then tilted sample stage by 60° so that the sample was set to be perpendicular to the ion beam and the sample was milled along the ac-plane of the multi layered thin film (as shown in figure 7.1 (d)).

The four probe technique and low pass filters in signal line are used for electrical characterization in current biasing mode. We use Keithley 6221 AC & DC current source and nano voltmeter 2182A for resistance vs temperature (R-T) characteristics and current vs voltage (I-V) measurement. A coaxial line from Wiltron sweep generator to the sample is used to supply the microwave.

7.3 Results and discussions

Figure 7.2 (a) shows FIB image (scale bar 1 μm) of device along with schematic. The device is fabricated on all a-axis oriented Y123/Pr123 multi layered thin films. The layered structure of Y123 and Pr123 give the phenomenon of Josephson junctions when

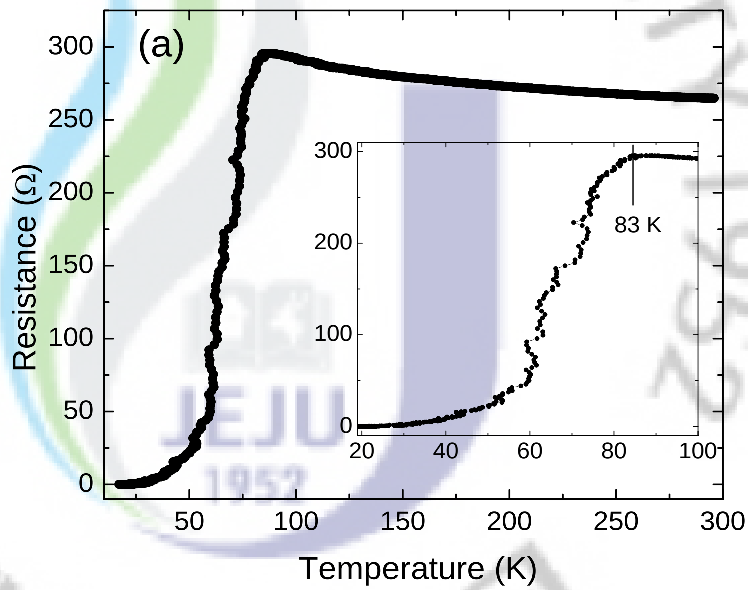

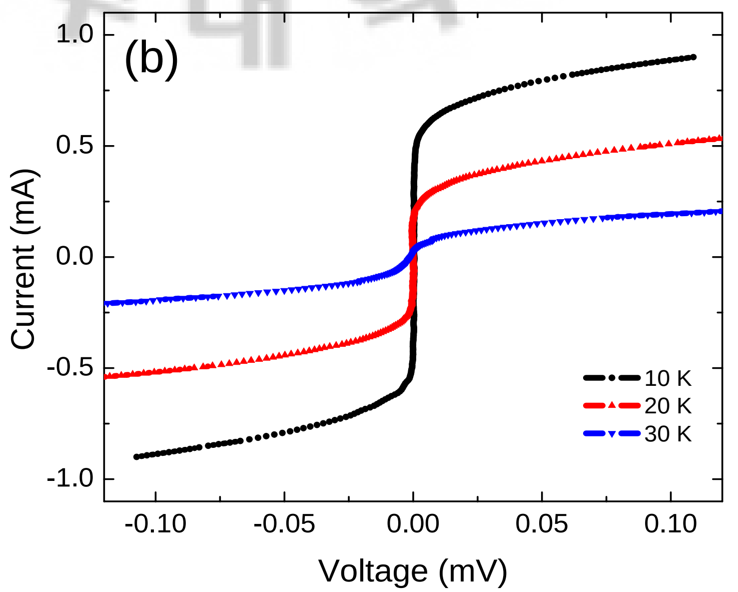

Fig. 7.3: (a) R-T characteristics of the device shows T_c about 83 K; (b) I-V characteristics of the device with out microwave irradiation at diffrent temperature of 10, 20, 30 K.

the current flows across the multi layered thin films (a-axis of thin films). Figure 7.2 (b) shows the detail description of device. The device has two submicron stacks of Josephson junctions with a submicron-loop of dimensions about 300 nm $\times$ 200 nm. The width of device is about 200 nm. The length of submicron stacks are different (200 nm and 100 nm) which is because of fabrication process. The red circle is magnified in next schematic figure 7.2 (c) which shows the layered structure of Y123 and Pr123 in submicron stack. The perpendicular red lines indicate CuO planes of Y123 and Pr123 thin films.

Figure 7.3 (a) shows R-T characteristics for the device. The value of transition temperature (T_c) about 83 K is observed. The value of critical current density (J_c) about 2×10^6 A/cm^2 at 20 K was estimated from I-V characteristics for the device without any external microwave irradiation. Figure 7.3 (b) shows I-V characteristics at different temperatures from 10 to 30 K. The device shows resistively shunted-junction (RSJ) characteristics below transition temperature also we did not observed any branch structure or hysteresis in I-V characteristics. The critical current suppresses with increase in temperature.

Figure 7.4 (a) shows the microwave power dependence of I-V characteristics at 20 K. The microwave of frequency 10 GHz is introduced by a coaxial cable. The voltage steps are observed in the flux flow (FF) type I-V characteristics caused by the Josephson vortices-flow in the junctions. These steps are more clear at high voltage and high microwave power. The inset of figure 7.4 (b) shows the magnified region at high microwave power with a voltage step.

The superconducting branch is sensitive to the microwave power. The value of I_c suppress with increase in the microwave power. The microwave power was varied from 0 dbm to 15 dbm in the step of 2.5 dbm. The first step (V$_{s1}$) in I-V characteristics appears at 21 μV (for 2.5 dbm power), and then the step shifts towards higher voltage while showing a complicated change due to the interference of different resonant modes.

Figure 7.4 (b) shows V_s dependence on the microwave power P. The square point shows experimental data and solid line shows a linear fit of these data. We linear fitted the experimental data with two ranges, R1) $0 < P < 10$ and R2) $7.5 < P < 10$. The value of V_{s1} and V_{s2} increase proportionally to the microwave power (P) in both range. However, the rate dV_{s2}/dP is about 2 and 1.5 times higher than dV_{s1}/dP in first range and second range, respectively. This may be due to an increase in number of Josephson

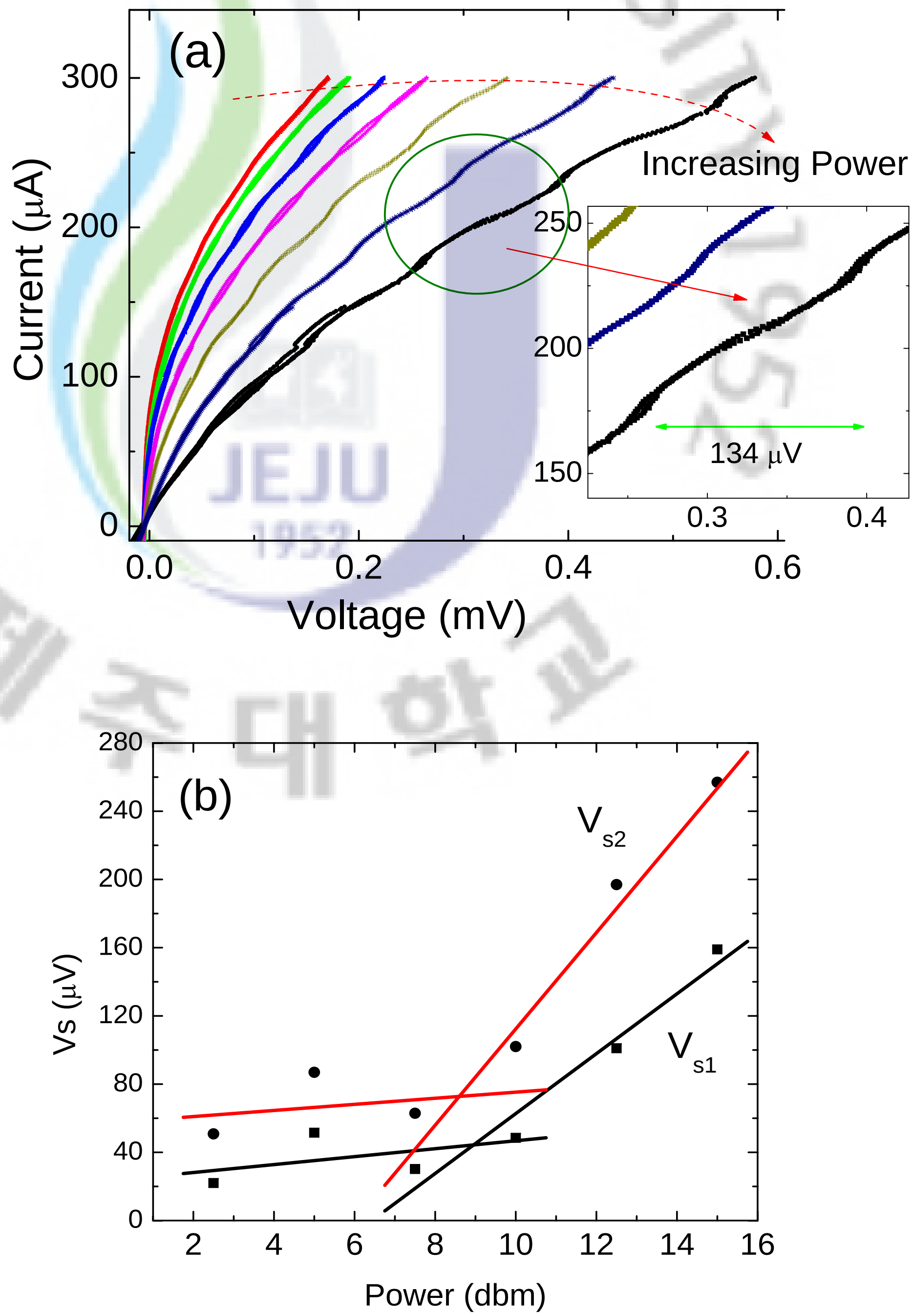

Fig. 7.4: (a) I-V characteristics of the device at 20 K with 10 GHz microwave irradiation of various power from 0 dbm to 15 dbm in the step of 2.5 dbm, inset shows the magnified area with a voltage step at high power; (b) Voltage steps dependence of power along with the linear fit for nano-SQUID at 20 K with 10 GHz microwave irradiation.

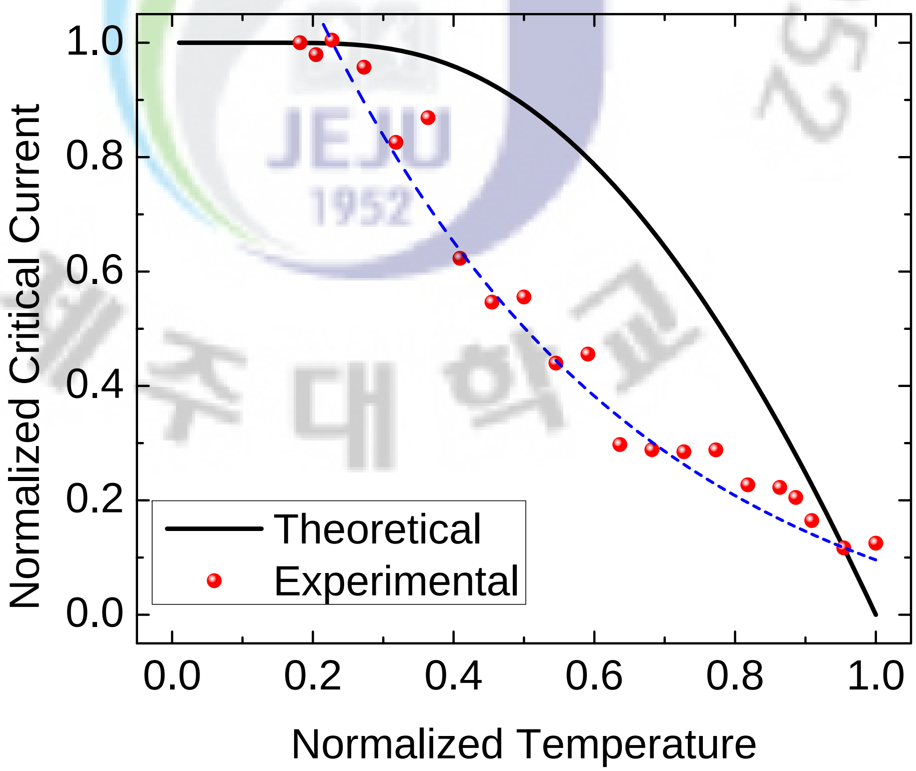

Fig. 7.5: The temperature dependence of normalized critical current ($I_c/I_{c\,at\ 10\ K}$) of the device. The broken line is guideline to the eyes.

junctions contributing to the vortices-flow. The difference in slope in first and second ranges may be due to the coupling of Josephson junctions with the microwave power.

The temperature dependence of normalized critical current ($I_c/I_{c\,at\,10K}$) is plotted in figure 7.5. The experimental data is compared with theoretical estimation of the Ambegaokar-Baratoff (A-B) theory [17]. The characteristics shows superconducting-semiconducting-superconducting (SSeS)-like Josephson junction which follows a good agreement with our experimental data. The results are similar as reported before for SSeS -like Josephson junctions [18]. We have successfully observed resonant like I-V characteristics of device under microwave irradiation.

7.4 Conclusions

We have grown the multi layered thin films of all a-axis oriented $YBa_2Cu_3O_7$ and $PrBa_2Cu_3O_7$ (Y123/Pr123) using pulsed laser deposition technique. The transition temperature (T_c) and critical current density (J_c) of multi layered thin film are about 83 K and 2×10^6 A/cm^2 at 20 K, respectively. A SQUID type structure device was fabricated using focused ion beam milling technique. The microwave induced voltage steps are observed in I-V characteristics. The super current branch become resistive above a certain microwave power and the value of J_c was suppressed as we increased the microwave power. The power dependence of voltage steps shows the number of Josephson junctions contributing to the vortices-flow varies with the power of microwave. The formation of superconducting-semiconducting-superconducting -like Josephson junction is confirmed by Ambegaokar-Baratoff theory.

BIBLIOGRAPHY

[1] S. Mahajan, J. G. Wen, W. Ito, Y. Yoshida, N. Kubota, C. -J. Liu, and T. Morishita, *Appl. Phys. Lett.* **65, 3129** (1994).

[2] Y. Shingai, M. Mukaida, K. Matsumo, Y. Yoshida, A. Ichinose, S. Horii, A. Saito, and S. Ohsima, *Physica C* **412, 1296** (2004).

[3] T. K. Worthington, W. J. Gallagher, and T. R. Dinger, *Phys. Rev. Lett.* **59, 1160** (1987).

[4] C. P.Foley and H. Hilgenkamp, *Supercond. Sci. Technol.* **22, 064001** (2009).

[5] S. Shapiro, *Phys. Rev. Lett.* **11, 80** (1963).

[6] S. Shapiro, A. Janus, and S. Holly, *Rev. Mod. Phys.* **36, 223** (1964).

[7] A. Irie, Y. Hirai, and G. Oya, **Appl. Phys.Lett. 72, 2159** (1998).

[8] C. H. Wu, Y. T. Chou, W. C. Kuo, J. H. Chen, L. M. Wang, J. C. Chen, K. L. Chen, U. C. Sou, H. C. Yang, and J. T. Jeng, *Nanotechnology* **19, 315304** (2008).

[9] M. Tachiki, T. Koyama, and S. Uchida, *Phys. Rev. B* **50, 7065** (1994).

[10] L. Ozyuzer *et al.*, *Science* **318, 1291** (2007).

[11] J. Bylander, T. Duty, and P. Delsing, *Nature* **434, 361** (2005).

[12] K. K. Likharev, *IBM J. Res. Develop.* **32, 144** (1998).

[13] A. Aassime, P. Delsing, and T. Claeson, *Nanotechnology* **12, 96** (2001).

[14] M. Takamura, M. Mukaida, S. Horii, A. Inchinose, R. Kita, K. Matsumoto, Y. Yoshida, M. Namba, S. Awaji, K. Watanabe, R. Teranishi, and N. Mori, *Supercond. Sci. Technol.* **23, 045023** (2010).

[15] S.-J. Kim, I. Yu. Latyshev, T. Yamashita, *Supercond. Sci. Technol.* **12, 729** (1999).

[16] S. Saini, G. S. Kim, S.-J. Kim, *J. Supercond. Nov Magn.* **23, 811** (2010).

[17] V. Ambegaokar and A. Baratoff, *Phys. Rev. Lett.* **10, 486** (1963).

[18] I. Takeuchi, P. A. Warburton, Z. Trajanovic, C. J. Lobb, Z. W. Dong, M. A. Bari, W. E. Booij, E. J. Tarte, and M. G. Blamire, *Appl. Phys.Lett.* **69, 112** (1996).

8. SUMMARY

The application of Josephson effect is always being focused by scientists and engineers. This thesis gives a flavour of application of Josephson effects in submicron range. Depending on lateral size, large Josephson junctions can be used as high frequency applications. The Josephson effect provides an unique principle to excite high-frequency electromagnetic (EM) wave in the single junctions or in arrays. The Josephson junctions can be used as the terahertz (THz) oscillator because of large superconducting gap. Although the emission from a single junction is weak and many junctions can emit high enough power for different applications. The solid-state THz radiation sources are useful for the applications in different fields such as medicine, diagnostics, bio-science, ultrahigh-speed communication, environmental studies, security systems, and nondestructive and noninvasive sensing and imaging.

The applications of submicron range Josephson junctions can be related with Coulomb blockade and effect of quantum phase fluctuations on cooper pair tunneling. The Josephson junctions shows an unique phenomenon when the size if sufficiently small so that the charge of a single electron matters. In quantum regime, the quantum conjugate properties of phase and number play an important role. The quantum regime can be observe when the value of charging energy is high enough to eliminate the thermal effect. In experimental point of view we took critical current density (J_c) which can be highly affected by both, thermal or quantum phase fluctuations. In this thesis, we showed that the possibility of quantum fluctuations which have suppressed the critical current density. This phenomenon have been achieved at 30 K. To observe this quantum effect we have fabricated stack of intrinsic Josephson junctions of $Bi_2Sr_2CaCu_2O_{8+\delta}$ (Bi-2212) whiskers of different in-plane areas (S) from 4 μm^2 down to 0.16 μm^2. The charging energy of the stack is increasing with decrease in in-plane area which lead to quantum fluctuations.

The presence of quantum fluctuations are verified with strong suppression in critical current density. The conditions to observe quantum effects are obeyed. The application of quantum effect can be use in a single electron device at 30 K.

Further extending the application of submicron Josephson junctions, we have studied the multi layered thin films of all a-axis oriented $YBa_2Cu_3O_7$ and $PrBa_2Cu_3O_7$ (Y123/Pr123) grown using pulsed laser deposition technique. The orientation of Y123 thin film can be controlled in any axis from a-axis to c-axis. Y123 can be a prospective candidate for nano device fabrication because of high T_c and higher value of critical current. A-axis oriented thin films are potentially superior to c-axis films for sandwich-type junction applications because of the larger coherence length in a-axis direction. Thus growth of thin epitaxial insulators or normal barriers on a-axis films, followed by another a-axis superconductor, is an important goal. Considering this phenomenon we have studied a submicron stack of Y123/Pr123 multi layered thin film Josephson junction. The submicron stack shows the transition temperature about 84 K and critical current of about 0.12 mA at 30 K. We notice suppression in critical current as the effect of external microwave at different power. As we increase the power, the superconducting state is suppressed and resulted in the suppression of the critical current. However, we have not observed voltage steps in current-voltage characteristics with external microwave irradiation which can be possibility of fabrication process. As during the fabrication process the Josephson junctions can be damaged.

With improving fabrication control, we fabricated a superconducting quantum interface device (SQUID) using focused ion beam milling technique. The microwave induced voltage steps are observed in I-V characteristics. The super current branch become resistive above a certain microwave power and the value of J_c was suppressed as we increased the microwave power. The power dependence of voltage steps shows the number of Josephson junctions which are contributing to the vortices-flow varies after a certain power of microwave. The formation of superconducting-semiconducting-superconducting like Josephson junction is confirmed by Ambegaokar-Baratoff theory.

Curriculum Vitae

Shrikant Saini

Graduate student
Jeju National University
Department of Mechanical Engineering
Engineering Building-4
Jeju, Republic of Korea 690756

Phone: +82-64-754-3715
Fax: +82-64-756-3886
Email: ssaini@jejunu.ac.kr
shrikantjnu@hotmail.com

Permanent Address

- 138, Kalyanpur Kalan,
  Kanpur, U.P.
  India
  Zip Code: 208017.

Personal

- Born on November 12, 1983.
- Kanpur, India.

Education

September 2007 - August 2011 **Ph.D.**, Department of Mechanical System Engineering, Jeju National University, Republic of Korea.

Ph.D. degree Project: A study of high-T_C superconductor submicron Josephson junction devices.

August 2003 - July 2005 **M.Sc.** Physics (6.23 out of 9), Jawaharlal Nehru University, New Delhi, India.

M.Sc. Thesis Title: Preparation and electromagnetic characterization of superconducting MgB_2

July 2000 - June 2003 **B.Sc.** Physics, Chemistry, and Mathematics (71%), C.S.J.M. University (P.P.N. Degree College), Kanpur, India.

Employment

March 2011 - June 2011 September 2009 - December 2009 and September 2008 - December 2008	**Teaching Assistant** under the guidance of **Prof. Sang -Jae Kim** Department of Mechatronics, Jeju National University, Jeju, Republic of Korea.
December 2005 - August 2007	**Project Associate** under the supervision of **Prof. R.C. Budhani** Department of Physics, Indian Institute of Technology, Kanpur, India.

Laboratory Experience

September 2007 - Onwards	**Nano Materials and System Laboratory**, Jeju National University, Republic of Korea.
December 2005 - August 2007	**Condensed Matter Low Dimension System Laboratory**, Indian Institute of Technology, Kanpur, India.
July 2004 - November 2005	**Condensed Matter Material Science Laboratory**, School of Physical Sciences, Jawaharlal Nehru University, New Delhi, India.

Publications

Journal Articles

1. **S. Saini**, Yuri Latyshev, and S.-J. Kim,*Investigation of critical current density of submicron intrinsic Josephson junctions of* $Bi_2Sr_2CaCu_2O_{8+\delta}$ *at 30 K*, Superconductor Science and Technology **24**, 075027 2011.

2. **S. Saini**, M. Takamura, M. Mukaida, and S.-J. Kim,*Electrical characterization of a-axis oriented Y123 thin film grown using pulsed laser deposition*, Accepted for publication in Current Applied Physics.

3. **S. Saini**, M. Takamura, M. Mukaida, and S.-J. Kim, *Microwave dependence of a-axis oriented* $YBa_2Cu_3O_7$ *thin film*, Accepted for publication in IEEE Transactions on Applied Superconductivity.

4. S. Chaudhari, N. K. Pandey, **Shrikant Saini**, and R. C. Budhani, *Dynamics of a robust photo-induced insulator-metal transition driven by coherent and broad-band light in epitaxial films of* $La_{0.625-y}Pr_yCa_{0.375}MnO_3$, Journal of Physics: Condensed Matter **22**, 275502 2010.

5. **Shrikant Saini**, Gui Shik Kim, and Sang-Jae Kim, *Suppression of Critical Current in Submicron Intrinsic Josephson Junction Fabricated in a* $Bi_2Sr_2Ca_2Cu_3O_{10+\delta}$ *Single Crystal Whisker*, Japanese Journal of Applied Physics **49**, 04DJ13 2010.

6. **S. Saini**, G.S. Kim, and S.-J. Kim, *Characterization of Submicron Sized Josephson junction Fabricated in a* $Bi_2Sr_2Ca_2Cu_3O_{10+\delta}$ *(Bi-2223) Single Crystal Whisker*, Journal of Superconductivity and Novel Magnetism **23**, 811 2010.

7. V. Gunasekaran, **S. Saini**, G.S. Kim, and S.-J. Kim, *Anomalous Change of Transport Characteristics of Graphite Planar-Type Micro-structures Fabricated by Focused Ion Beam*, Journal of Superconductivity and Novel Magnetism **23**, 1193 2010.

8. H.-S. Lee, J.-H. Park, J.-Y. Lee, J.-Y. Kim, N.-H. Sung, T.-Y. Koo, B. K. Cho, C.-U. Jung, **S. Saini**, S.-J. Kim and H.-J. Lee, *High-pressure growth of fluorine-free $SmFeAsO_{1-x}$ superconducting single crystals*, Journal of Superconductor Science and Technology **22**, 075023 2009.

9. **Shrikant Saini** and S.-J. Kim, *Growth of $Bi_2Sr_2Ca_2Cu_3O_{10+\delta}$(Bi-2223) Single Crystal Whiskers*, IEEE Transactions on Applied Superconductivity **19** NO. 3, 3030 2009.

Proceedings

1. **S. Saini**, Venugopal Gunasekaran and S. J. Kim, *Characterization of intrinsic Josephson junction stack using high-T_c superconducting $Bi_2Sr_2CaCu_2O_{8+\delta}$*, The Korea Institute of Applied Superconductivity and Cryogenics **978-89-957138-2-2**, 1007 2009.

2. V. Gunasekaran, **S. Saini**, G. S. Kim, and S. J. Kim, *Electrical Transport Measurements of Graphite flakes for Microelectronic Device Applications*, The Korea Institute of Applied Superconductivity and Cryogenics **978-89-957138-2-2**, 1025 2009.

3. **S. Saini** and S. J. Kim, *Transport characteristics of $Bi_2Sr_2Ca_2Cu_3O_{10+\delta}$ (Bi-2223) single crystal whisker*, Journal of Physics: Conference Series **150**, 052109 2009.

Domestic Journals

1. **S. Saini**, G.-S. Kim, and S.-J. Kim, *Fabrication of Nano-Periodic Josephson Junction Array in Submicorn area of $Bi_2Sr_2CaCu_2O_{8+\delta}$ (Bi-2212)*, Jeju National University Research Institute of Advance Technology Journal **20**, 29 2009.

Presentations

International Conferences

1. **S. Saini**,M. Takamura, M. Mukaida, and S.-J. Kim, *Fabrication of Nano SQUID in Multilayered Thin Film of Y123/P123 using Focused Ion Beam*, The 23^{rd} International Microprocesses and Nanotechnology Conference, Kokura Japan, November 2010.

2. **S. Saini**, M. Takamura, M. Mukaida, and S.-J. Kim, *Josephson junction fabrication in multilayered Y-123/Pr-123/Y-123 thin film*, International Union of Materials Research Societies International Conference on Electronic Materials 2010, Seoul Republic of Korea, August 2010.

3. **S. Saini**, M. Takamura, M. Mukaida, and S.-J. Kim, *Fabrication of Josephson junction in a-axis oriented Y-123/Pr-123/Y-123 heterostrcutures using focused ion beam*, The 8^{th} International Nanotech Syamposium and Exhibition in Korea Joint Symposium with IEEE Nano 2010, Seoul Republic of Korea, August 2010.

4. **S. Saini** and S.-J. Kim, *Fabrication and electrical characterization of small capacitance intrinsic Josephson junction of* $Bi_2Sr_2CaCu_2O_{8+\delta}$ *whiskers*, The 8^{th} International Nanotech Syamposium and Exhibition in Korea Joint Symposium with IEEE Nano 2010, Seoul Republic of Korea, August 2010.

5. **S. Saini**, M. Takamura, M. Mukaida, and S.-J. Kim, *Microwave dependence of a-axis oriented* $YBa_2Cu_3O_7$ *thin film*, Applied Superconductivity Conference 2010, Washington D.C. United States of America, August 2010.

6. **S. Saini** and S.-J. Kim, *Experiment evidence of quantum fluctuation at 30 K in submicron area of* $Bi_2Sr_2Ca_2Cu_3O_{10+\delta}$ *(Bi-2223) single crystal whiskers*, Applied Superconductivity Conference 2010, Washington D.C. United States of America, August 2010.

7. **<u>S. Saini</u>**, M. Takamura, M. Mukaida, and S.-J. Kim, *Electrical characterization of a-axis oriented Y123 thin film grown using pulsed laser deposition*, The 10^{th} Asia Pacific conference on Plasma Science and Technology and 23^{th} Symposium on Plasma Science for Materials, Jeju Republic of Korea, July 2010.

8. **<u>S. Saini</u>**, M. Takamura, M. Mukaida, and S.-J. Kim, *Transport properties of submicron stack of Y123/Pr123 multilayered thin film* , The 7^{th} Asian Meeting on Ferroelectricity and 7^{th} Asian Meeting on ElectroCeremics, Jeju, Republic of Korea, June 2010.

9. **<u>S. Saini</u>**, M. Takamura, M. Mukaida, and S.-J. Kim, *Electric Transport Properties along the a-axis of Y123/Pr123 multilayered thin film in submicron area*, The 7^{th} International Symposium on Intrinsic Josephson Effects and Plasma Oscillations in High T_c Superconductors, Hirosaki Japan, April 2010.

10. **<u>S. Saini</u>** and S.-J. Kim, *In-plane Area Dependence of Nano-periodic Joseohson Junction Array*, The 6^{th} International Conference on Advanced Materials and Devices, Jeju, Republic of Korea, December 2009.

11. **<u>S. Saini</u>** and S.-J. Kim, *Fabrication of Nano-scale Stack of* $Bi_2Sr_2Ca_2Cu_3O_{10+\delta}$ *(Bi-2223) Single Crystal Whisker*, International Conference on Nano Science and Nano Technology, Mokpo, Republic of Korea, November 2009.

12. **<u>S. Saini</u>** and S.-J. Kim, *Suppression of critical current in submicron intrinsic Josephson junction fabricated in a* $Bi_2Sr_2Ca_2Cu_3O_{10+\delta}$ *(Bi-2223) Single Crystal Whisker*, International conference on Solid State Devices and Materials, Miyagi Japan, October 2009.

13. S.-J. Kim and **<u>S. Saini</u>**, *Fabrication of Three terminal devices in* $Bi_2Sr_2CaCu_2O_{8+\delta}$ *(Bi-2212) using focused ion beam (FIB) etching methods*, The 9^{th} International Conference on Materials and Mechanisms of Superconductivity, Tokyo Japan, September 2009.

14. **S. Saini** and S.-J. Kim, *Electrical Transport Properties of Nano-Periodic Josephson Junction Array of* $Bi_2Sr_2Ca_2Cu_3O_{10+\delta}$ *(Bi-2223) Single Crystal Whisker*, The 9th International Conference on Materials and Mechanisms of Superconductivity, Tokyo Japan, September 2009.

15. **S. Saini** and S.-J. Kim, *Characterization of Submicron junction, fabricated in a* $Bi_2Sr_2Ca_2Cu_3O_{10+\delta}$ *(Bi-2223) Single Crystal Whisker*, Seventh International Conference on New Theories, Discoveries and Applications of Superconductors and Related Materials, Beijing China, May 2009.

16. **S. Saini** and S.-J. Kim, *Nano-Periodic Josephson Junction Array Fabrication in* $Bi_2Sr_2Ca_2Cu_3O_{10+\delta}$ *(Bi-2223) single crystal whisker*,21st International Microprocesses and Nanotechnology Conference, Fukuoka Japan, October 2008.

17. **S. Saini** and S.-J. Kim, *Transport characteristics of* $Bi_2Sr_2Ca_2Cu_3O_{10+\delta}$ *(Bi-2223) single-crystal whisker*, 25th International Conference on Low Temperature Physics, Amsterdam The Netherlands, August 2008.

18. **S. Saini** and S.-J. Kim, *Growth of* $Bi_2Sr_2Ca_2Cu_3O_{10+\delta}$ *(Bi-2223) single crystal whiskers*, Applied Superconductivity Conference 2008, Chicago United States of America, August 2008.

19. **S. Saini** and S.-J. Kim, *Characterization Of Intrinsic Josephson Junction Stack Using High-*T_c *Superconducting* $Bi_2Sr_2CaCu_2O_{8+\delta}$ *(Bi-2212)*, International Cryogenic Engineering Conference 22nd and International Cryogenic Materials Conference, Seoul Republic of Korea, July 2008.

20. **S. Saini** and S.-J. Kim, *Growth of single phase* $Bi_2Sr_2Ca_2Cu_3O_{10+\delta}$ *(Bi-2223) single crystal whisker*, The 6th International Symposium on Intrinsic Josephson Effect and Plasma Oscillations in High-T_c Superconductors, Pohang Republic of Korea, July 2008.

Domestic Conferences

Many conferences orginaized by the Korean Physical Society, the Korean superconductivity society, the Korean society of precision engineering, the Korean society of mechanical engineering, and the Korean vacuum society.

Computer Skill

- Labview
- Latex
- OriginPro 7.5

Broad areas of interest

- Superconductivity
- Josephson Junction
- Focused Ion Beam
- Strongly correlated systems
- Nano Devices

Techniques and Instruments Skill

- Focused Ion Beam (SII NanoTechnology SMI2050) for *fabrication of submicron devices*
- Close cycle refrigerator 10 K
- Exchange type close cycle refrigerator 4.2 K
- Cryogen free low temperature 1.6 K and 8 T magnetic field Cryogenics Inc., U.K.
- Wiltron sweep generator for external microwave irradiation up to 40 Ghz
- Pulse Laser Deposition

- Thermal Deposition Chamber
- Veeco Dektak 6M Stylus Profiler
- Lithography
- Ar Ion Milling Setup

Travel History

August 1, 2010 - August 7, 2010	**Washington DC, USA** to attend Applied Superconductivity Conference 2010 in Omni Shoreham Hotel.
May 13, 2009 - May 17, 2009	**Beijing, China** to attend Seventh International Conference on New Theories, Discoveries and Applications of Superconductors and Related Materials in Double Tree - Hilton hotel.
August, 2007 - Onwards	**Jeju, Republic of Korea** to pursue Ph.D. in Department of Mechanical System Engineering, Jeju National University, Jeju, Republic of Korea.

Society Member

- Korean Physical Society, Korea.
- Korean Superconductivity Society, Korea.
- Institute of Physics, U.K.
- American Physical Society, USA.